Life Science Informatics Publications

Research Journal of Life Sciences, Bioinformatics, Pharmaceutical and Chemical Sciences

Journal Home page http://www.rjlbpcs.com/

RJLBPCS

ISSN 2454-6348

Original Research Article **DOI: 10.26479/2025.1101.02**

COMPUTATIONAL & SYSTEM BIOLOGY APPROACHES IN IDENTIFYING POTENTIAL NATURAL PLANT BASED COMPOUNDS IN COMBATING PANCREATIC CANCER

Ariba Anwar[1,2], Viswa Raj Lal[2], Harsimran Kaur Hora[1], Priyangulta Beck[1], Mukesh Nitin[1*]

1. Dept. of Tech Biosciences, Digianalix, Ranchi, Jharkhand, INDIA.

2. Dept. of Biotechnology, Jamshedpur Women's University, Jamshedpur, Jharkhand, INDIA.

ABSTRACT: Pancreatic cancer remains a formidable challenge due to late diagnosis and limited treatment options. This study utilized bioinformatic tools to identify potential therapeutic candidates from natural sources. We analyzed five gene expression datasets from GEO2R to identify differentially expressed genes (DEGs). A total of 249 commonly deregulated genes were identified, and subsequent network analysis highlighted EGF and FOXO3 as key hub genes. EGF promotes tumor growth, while FOXO3 regulates cell cycle arrest and apoptosis. To identify natural modulators of these targets, we curated a compound library from PubChem. In silico screening using DruLito and Osiris evaluated the drug-likeness and potential toxicity of these compounds. Finally, molecular docking simulations assessed the binding affinity of 15 shortlisted compounds with EGF and FOXO3. Pheophorbide A and curcumin emerged as promising candidates, demonstrating binding affinities of -6.5 kcal/mol and -6.9 kcal/mol for EGF and FOXO3, respectively. These findings suggest that targeting these critical regulators with natural products could provide a novel therapeutic strategy for pancreatic cancer by disrupting cancer cell proliferation and survival mechanisms.

Keywords: Pancreatic Cancer, EGF, FOXO3, Bioinformatics, Molecular Docking, Natural Compounds.

Article History: Received: Jan 10, 2025; Revised: Jan 12, 2025; Accepted: Feb 10, 2025.

Corresponding Author: Dr. Mukesh Nitin* Ph.D.

Department of Tech Biosciences, Digianalix, Ranchi, Jharkhand, India.

E-mail Address: digianalix@gmail.com

1. INTRODUCTION

Pancreatic cancer, with one of the highest mortality rates among all malignancies, is the seventh leading cause of global cancer-related deaths [1]. According to GLOBOCAN 2020, pancreatic cancer is the 12th most common cancer (2.6% of all cancers) and is the 7th leading cause of global cancer deaths at 4.7% [2]. Rising mortality rates could make this the second leading cause of cancer deaths by 2030 [3]. This malignancy often presents minimal to no symptoms until reaching an advanced stage [4]. Clinically, pancreatic cancer refers to a malignant tumor originating from the epithelial cells of the pancreatic ductal glands, commonly known as adenocarcinoma [5]. Pancreatic ductal adenocarcinoma (PDAC) comprises over 90% of pancreatic cancer cases [6]. It is challenging to treat because it often presents at a late, inoperable stage and exhibits significant resistance to both cytotoxic and targeted molecular therapies [7]. In 2020, the 5-year survival rate for pancreatic cancer rose to 10%, up from 5.26% in 2000 [8]. Surgical resection is possible for less than 20% of pancreatic cancer patients, offering a potential cure. However, median survival is under 2 years, with 80% recurrence. Around 12% survive 5 years, depending on cancer stage, grade, and tumor factors [9, 10]. Currently, pancreatic cancer remains a challenge, with prognosis showing minimal improvement over the past 20 years [11]. Gemcitabine stands as the primary chemotherapeutic agent in treating advanced pancreatic cancer [12,13,14]. Yet, conventional chemotherapy and radiation have not improved five-year survival rates [15,16]. Research indicates that FOLFIRINOX improves survival rates in patients, but it is accompanied by increased treatment-related toxicity [17]. Despite effective precision therapies for other cancers like breast and ovarian, PDAC has limited options, with erlotinib as the only approved agent offering minimal survival benefit [18,19]. Despite chemotherapy advances, further understanding of PDAC's molecular mechanisms and identification of new therapeutic targets is urgently needed to improve patient outcomes. Identifying potential targets for pancreatic cancer treatment involves studying genes and pathways linked to patient prognosis, essential for understanding PDAC's aggressiveness [9]. In our studymicroarray gene expression analysis was performed to pinpoint genes or gene signatures correlated with pancreatic cancer [20,21,22]. Using bioinformatic approaches and high-throughput genomic technologies like microarray data, we analyzed PDAC and normal pancreatic tissues to identify key genes and pathways, revealing hub genes like EGF and FOXO3 critical in PDAC progression and resistance. EGFR inhibitors have had limited success in PDAC clinical trials, except for erlotinib and nimotuzumab, highlighting resistance mechanisms and the need for alternative therapies. Combining them with multi-targeted drugs may offer better outcomes [23]. In pancreatic cancer, the PI3K/Akt pathway remains persistently activated [24,25,26]. A promising anti-cancer drug design strategy involves targeting FOXO3a through the PI3K-PKB pathway and influencing its co-activators or corepressors to regulate its function in cancer cells [27]. The application of precision oncology with the exploration of natural compounds as drug candidates is anticipated to improve

PDAC treatment efficacy and reduce toxicity. Using bioinformatics and gene expression data, we aim to identify natural compounds targeting key proteins, potentially disrupting cancer progression. This research highlights the significant potential of natural compounds in cancer therapy and the crucial role of bioinformatics in accelerating drug discovery.

2. MATERIALS AND METHODS

2.1. Data Acquisition

Gene expression profiles for pancreatic cancer were obtained from the Gene Expression Omnibus (GEO) database (https://www.ncbi.nlm.nih.gov/geo/) using the keyword "Pancreatic Cancer." The results were filtered by selecting "Datasets," "Homo sapiens," and "Expression Profiling by Array" as filters. This search yielded 18 datasets, of which five gene expression microarray datasets—GSE16515, GSE28735, GSE18670, GSE57728, and GSE19650—were selected for differential expression gene (DEG) analysis.

Case 1 (GSE16515) comprised 36 tumor samples and 16 normal samples, totaling 52 samples. Case 2 (GSE28735) contained 45 matching pairs of pancreatic tumor and adjacent non-tumor tissues from 45 patients with pancreatic ductal adenocarcinoma (PDAC), totaling 90 samples. Case 3 (GSE18670) compared circulating tumor cells (CTCs) with hematological cells (G), original tumor (T), and non-tumor pancreatic control tissue (P). This dataset aimed to develop a gene signature for CTCs and assess the survival of patients after surgical resection for pancreatic cancer. Case 4 (GSE57728) demonstrated the effectiveness of the CREB-binding protein inhibitor ICG-001 in suppressing pancreatic cancer cell growth by treating AsPC1 cells. Case 5 (GSE19650) focused on multistep pancreatic carcinogenesis by comparing gene expression profiles of normal main pancreatic duct cells with those from intraductal papillary-mucinous adenoma (IPMA), intraductal papillary-mucinous carcinoma (IPMC), and intraductal papillary-mucinous neoplasm (IPMN). The study observed that as IPMA progresses to IPMC, the host's immune response shifts from activation to tolerance.

2.2. Identification and Analysis of Differentially Expressed Gene

Differentially Expressed Genes (DEGs) were acquired using the GEO2R tool available in the GEO database [28]. It uses the GEOquery and limma R packages from the Bioconductor project to compare different groups of samples in the GEO dataset. Tumor samples were designated as the test group and normal samples were the control group. Gene expression profiles of the pancreatic cancer (PC) groups were individually compared with those of the normal groups within each dataset. Normalization was performed using the RMA algorithm. The Benjamini-Hochberg (BH) [29] adjustment was applied to detect DEGs between tumor and normal tissues, and to eliminate the False Discovery Rate(FDR). Volcano, mean, and box plots were obtained from the GEO2R analysis. The table for differentially expressed genes was downloaded, and genes were sorted with a P-value threshold of <0.05.The DEGs were then further analyzed for gene conservancy using the Venn Gene

tool (https://bioinformatics.psb.ugent.be/webtools/Venn/), which creates Venn diagrams for Bioinformatics and Evolutionary Genomics. This tool combines datasets to identify overlapping DEGs or highly significant genes conserved across all cases.

2.3. Protein-protein interaction (PPI) network construction and Bioinformatic analysis of DEGs

Cytoscape software v3.10.2 was employed for network analysis and visualization of candidate DEGs encoding proteins associated with pancreatic cancer. Several Cytoscape plugins were used in the analysis: STRINGApp to construct the Protein-Protein Interaction (PPI) network for metabolic pathways, CytoHubba to identify the top 10 hub genes or nodes within the PPI network using the Degree method, and yFiles Layout Algorithms, particularly the Hierarchic Layout for Selected Nodes, to arrange networks into hierarchical layers and reorganize sub-graphs for enhanced clarity in visualization.

2.4. Physicochemical Characterization

To obtain the protein sequences in FASTA canonical format for the two selected hub genes, EGF and FOXO3, the UniProt database (https://www.uniprot.org/) was used. Physicochemical properties, including amino acid composition, molecular weight, pI, the total number of negatively and positively charged residues, extinction coefficient, instability index, aliphatic index, and the grand average of hydropathicity (GRAVY), were computed using the ProtParam tool [30].

2.5. Secondary structure prediction and functional characterization

The secondary structure prediction of the protein was conducted using SOPMA (Self-Optimized Prediction Method with Alignment) [31]. Additionally, SOSUI [32] was employed to predict transmembrane regions in protein sequences and to classify proteins as either membrane-bound or soluble.

2.6. Homology Modelling, Evaluation and Receptor preparation

The three-dimensional (3D) structure of the protein was obtained by submitting its amino acid sequences to SWISS-MODEL [33], an automated server for protein structure homology modeling. This tool automates template selection, alignment, and model building. The quality of the raw homology model was initially evaluated using the Procheck server. A Ramachandran plot was utilized to analyze protein structures and assess the precision of the model, particularly focusing on backbone dihedral angles and overall geometry. Accordingly, Procheck UCLA [34] and Ramachandran plot analyses were performed to validate the stereochemical quality of the protein structures.

Receptor preparation for EGF and FOXO3 was carried out using UCSF Chimera [35] by selecting chain A of the protein and removing any ions, ligands, or solvents. Swiss-PdbViewer [36] was employed for energy minimization, and the refined structure was saved as the current layer in PDB format. UCSF Chimera was then used again for structure editing, including adding hydrogens and

charges. In the Surface/Binding Analysis tool, the "Dock Prep" option was selected to prepare the receptor for docking studies.

2.7. Ligand library construction and screening

Active natural compounds were selected through a scientific literature survey. The PubChem [37] library was screened for natural compounds capable of actively targeting the selected receptors. All screened compounds were downloaded from PubChem in 3D SDF format. DruLiTo and OSIRIS software were employed for ADMET analysis. DruLiTo was used to calculate drug-likeness properties using the Lipinski filter [38], while the OSIRIS [39] Property Explorer was utilized to predict and evaluate toxicity profiles and risk factors such as mutagenicity, tumorigenicity, irritancy, and reproductive effects. These analyses facilitated the selection of compounds with favorable drug-like properties.

2.8. Ligand Preparation

Based on criteria such as drug-likeness, toxicity profile, and pharmacokinetics, compounds were selected for preparation. The 3D SDF structures of the selected ligands were imported into Avogadro [40] software, where the force field was set to GAFF (General Amber Force Field). Geometry optimization was conducted with 5000 steps to refine the ligand structures, resulting in energy-minimized forms suitable for docking studies. These files were then converted to PDB format using Avogadro. For the final ligand preparation of the selected compounds, UCSF Chimera was employed. Structure editing involved adding hydrogens and charges, and the files were saved in PDB format for molecular docking.

2.9. Molecular Docking

Docking of the ligands with the target receptor was performed using AutoDock Vina in Chimera. In docking simulations, good scores are those that are negative and have large absolute values. Thus, receptor-ligand interactions with the lowest score or free binding energy (ΔG) were prioritized, as these indicate the stability of the bound complex. After docking, the receptor-ligand PDBQT input files were generated automatically. Open Babel [41] was then used to convert the PDBQT files to PDB format. Based on docking results, compounds with high binding affinities and favorable binding modes were screened as potential drug candidates. Receptor-ligand interactions were visually analyzed using Biovia Discovery Studio software [42], which identified hydrogen bonds, hydrophobic interactions, and other relevant interactions in each docked pose.

3. RESULTS AND DISCUSSION

3.1. Identification of differentially expressed genes and Meta-Analysis

In this study, five gene expression profiling microarray datasets, representing five different cases of pancreatic cancer, were selected and analyzed individually. The analysis was conducted using the online tool GEO2R to identify Differentially Expressed Genes (DEGs). Read normalization was

performed, with samples designated as test and control groups, prior to metagenomics analysis. The results are depicted as box plots, volcano plots, and MA plots (Fig. 1–3).

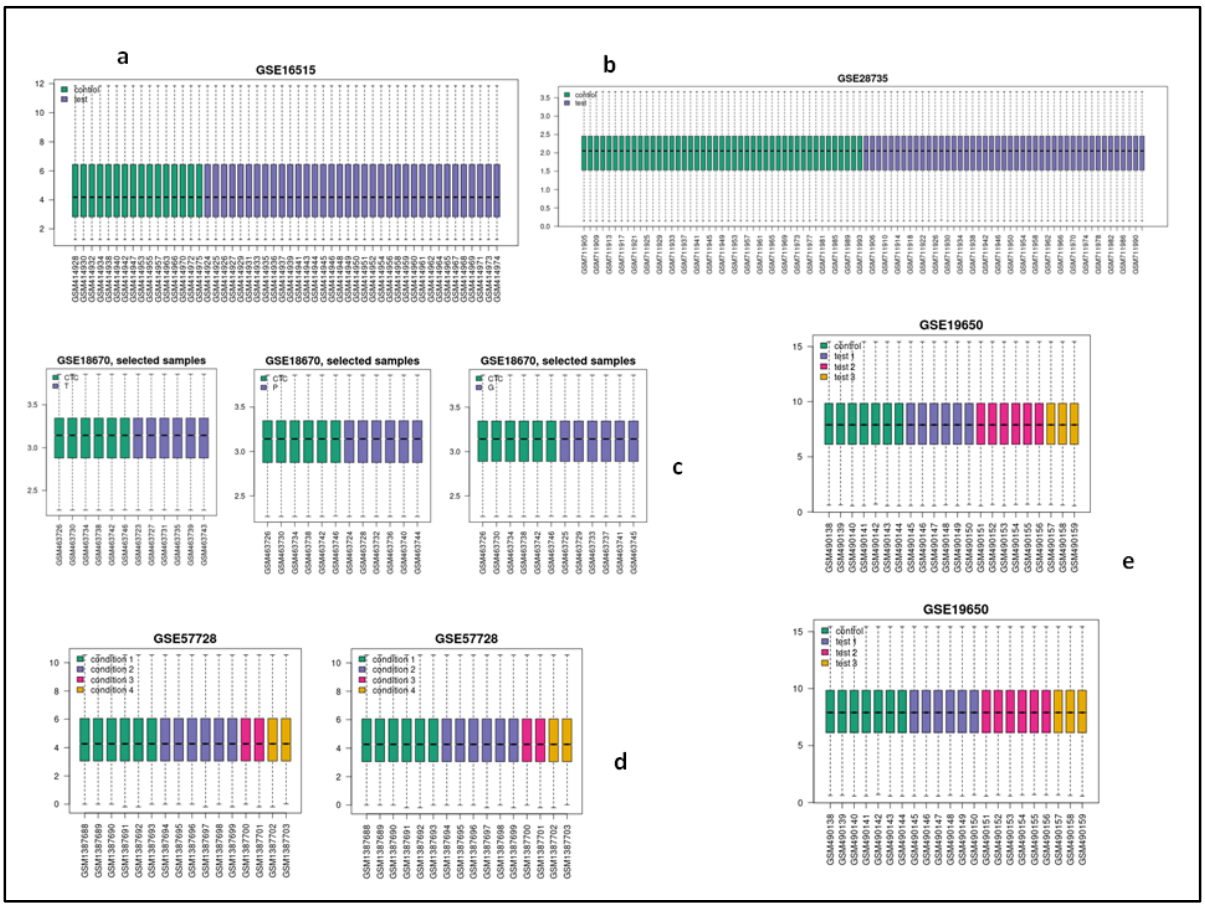

Fig. 1: Normalization plot obtained from geodatasets (a. GSE16515, b. GSE28735, c.GSE18670, d. GSE57728, e. GSE19650)

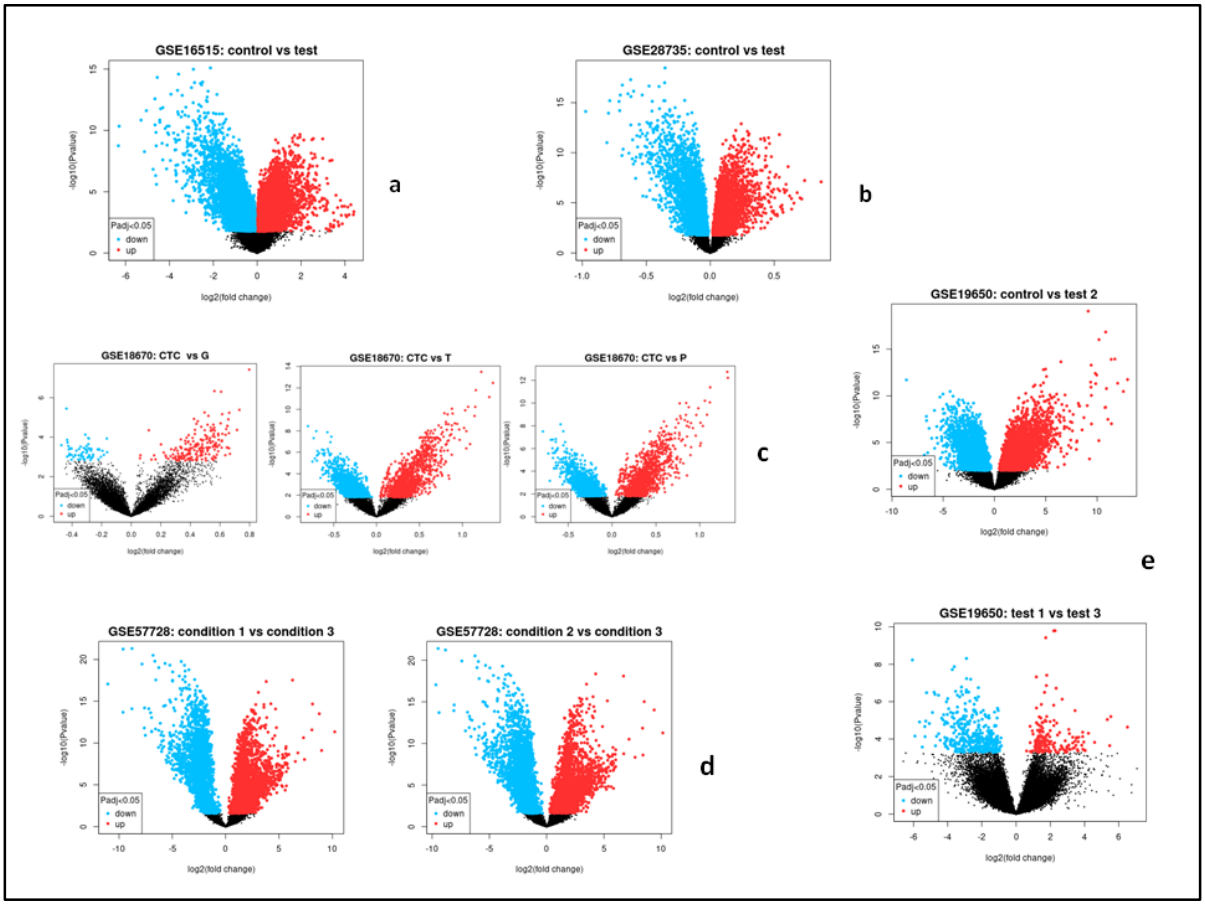

Fig. 2: Volcano plot obtained from Geo Datasets (a. GSE16515, b. GSE28735, c.GSE18670, d. GSE57728, e. GSE19650)

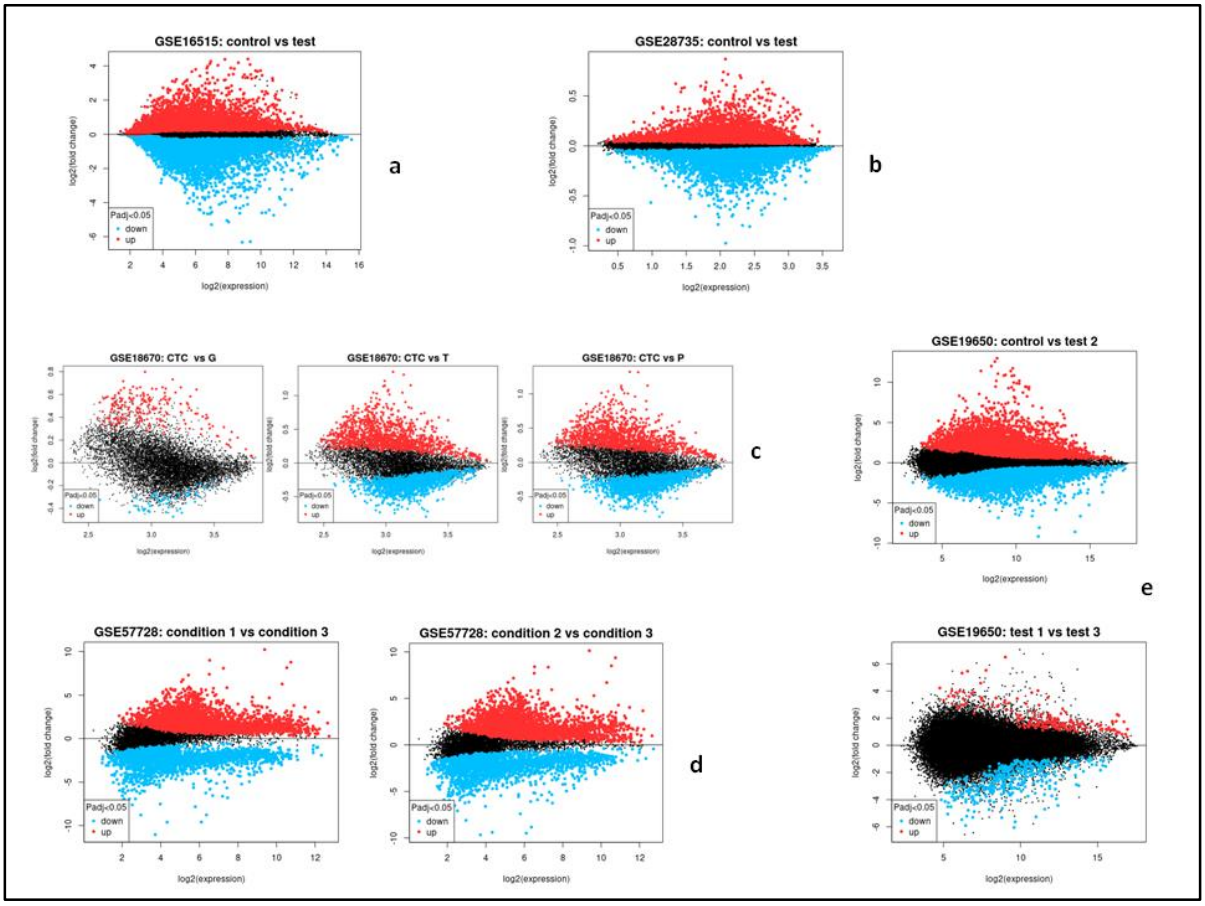

Fig. 3: MA plotobtained from Geo Datasets (a. GSE16515, b. GSE28735, c.GSE18670, d. GSE57728, e. GSE19650)

Differentially expressed genes for each case were identified using a p-value threshold of <0.05. In GSE16515 (case 1), 23,304 DEGs were identified by comparing 36 tumor samples with 16 normal samples. In GSE28735 (case 2), 12,109 DEGs were obtained by analyzing gene expression profiles from 45 pairs of pancreatic tumor and adjacent non-tumor tissues. Gene expression profiles from GSE18670 (case 3) revealed 9,143 DEGs when circulating tumor cells (CTCs) were compared with haematological cells (G), the original tumor (T), and non-tumorous pancreatic control tissue (P) derived from patients with pancreatic ductal adenocarcinoma (PDAC). Specifically, 2,003 DEGs were identified in CTC vs. G, 3,536 DEGs in CTC vs. T, and 3,604 DEGs in CTC vs. P. GSE57728 (case 4) identified 11,556 DEGs from AsPC1 cells treated with ICG-001, DMSO, and transfected with control siRNA and CTNNB1 siRNA at different time points. Finally, GSE19650 (case 5) identified 24,142 DEGs when the normal main pancreatic duct was used as a control and compared to three test groups: IPMA (test 1), IPMC (test 2), and IPMN (test 3).

Further analysis of DEGs across all five datasets revealed 249 conserved genes common to all cases, as shown in Fig. 4a. A Protein-Protein Interaction (PPI) network of these conserved genes, focused on metabolic pathways, was constructed using STRINGApp in Cytoscape. From this network, the

top 10 hub genes—EGF, PTEN, TGFB1, KRAS, CREBBP, PECAM1, FOXO3, H2BC21, FYN, and THBS1—were identified (Fig. 4b).

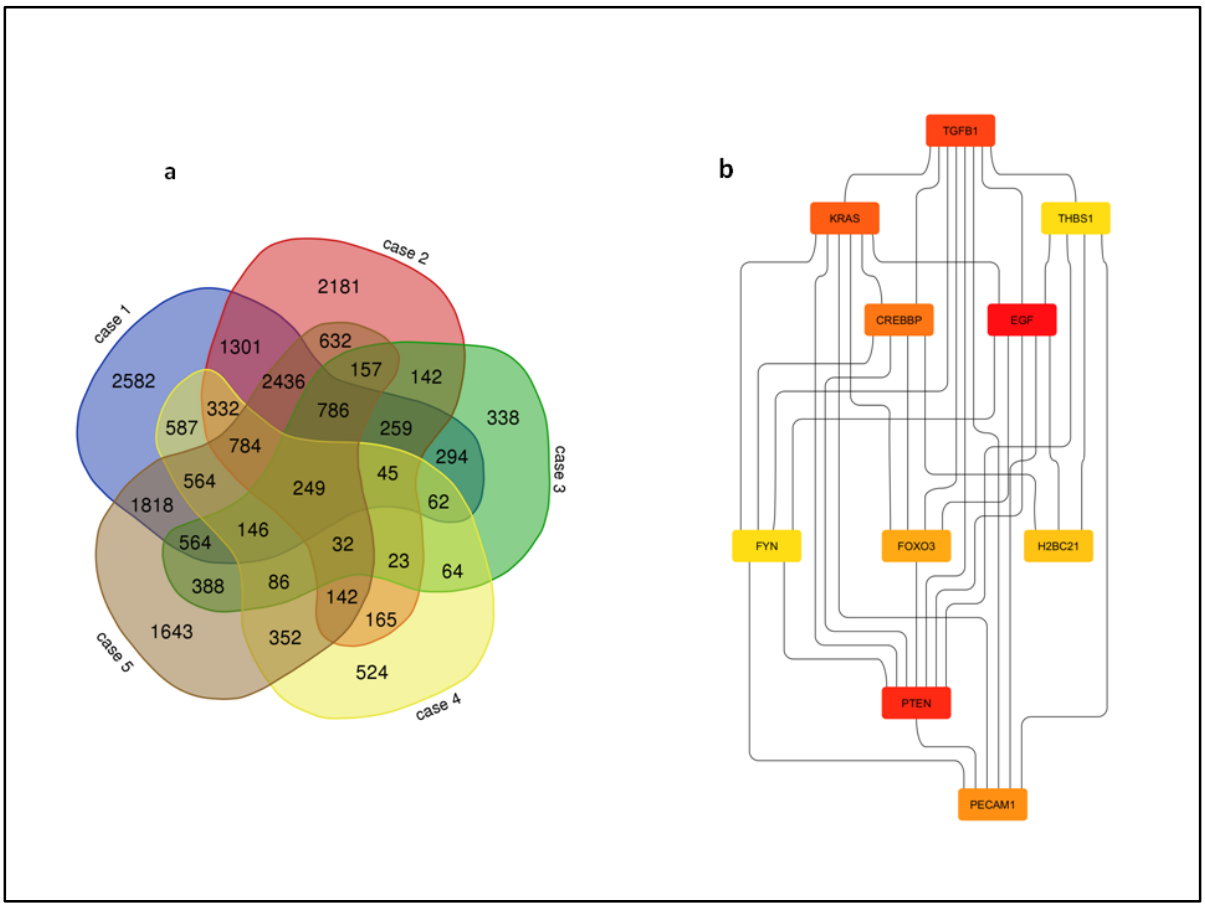

Fig. 4: (a) Venn diagram illustrating the overlapping number of Differentially Expressed Genes (DEGs) across various analyzed datasets. **(b)** PPI network of top ten hub genes obtained from string analysis

Based on a review of scientific literature, EGF and FOXO3 were selected for further analysis due to their critical roles in pancreatic cancer progression. EGF promotes tumor growth by activating key signaling pathways, while FOXO3 plays a vital role in regulating apoptosis and cell cycle control. Suppression of FOXO3 results in uncontrolled cell proliferation and survival. Thus, targeting these genes may disrupt cancer progression and improve therapeutic outcomes.

3.2. Receptor Analysis and Preparation

The ProtParam tool was used to analyze the physicochemical properties of the EGF and FOXO3 receptors by calculating relevant parameters. For EGF and FOXO3, the number of amino acids was found to be 1207 and 673, respectively. The theoretical pI values were 5.53 for EGF and 4.98 for FOXO3. The instability index values were 48.69 and 66.77, indicating the stability levels of the proteins, while the grand average of hydropathicity (GRAVY) values were -0.34 and -0.594, respectively, as shown in Table 1. Secondary structure predictions for EGF and FOXO3 were

performed using SOPMA, identifying elements such as alpha helices, beta turns, random coils, and others, as depicted in Figures 5 and 6. Protein classification was conducted using SOSUI, which identified EGF as a membrane protein and FOXO3 as a soluble protein, as shown in Figures 7 and 8.

Table 1: Protparam Results for physiochemical properties of EGF and FOXO3

EGF	**FOXO3**
Number of amino acids: 1207	Number of amino acids: 673
Molecular weight: 133994.17	Molecular weight: 71276.63
Theoretical Pi: 5.53	Theoretical Pi: 4.98
Instability Index (II): 48.69 This classifies the protein as unstable	Instability Index (II): 66.77 This classifies the protein as unstable
Aliphatic Index: 77.26	Aliphatic Index: 62.11
Grand average of hydropathicity (GRAVY): -0.304	Grand average of hydropathicity (GRAVY): -0.594

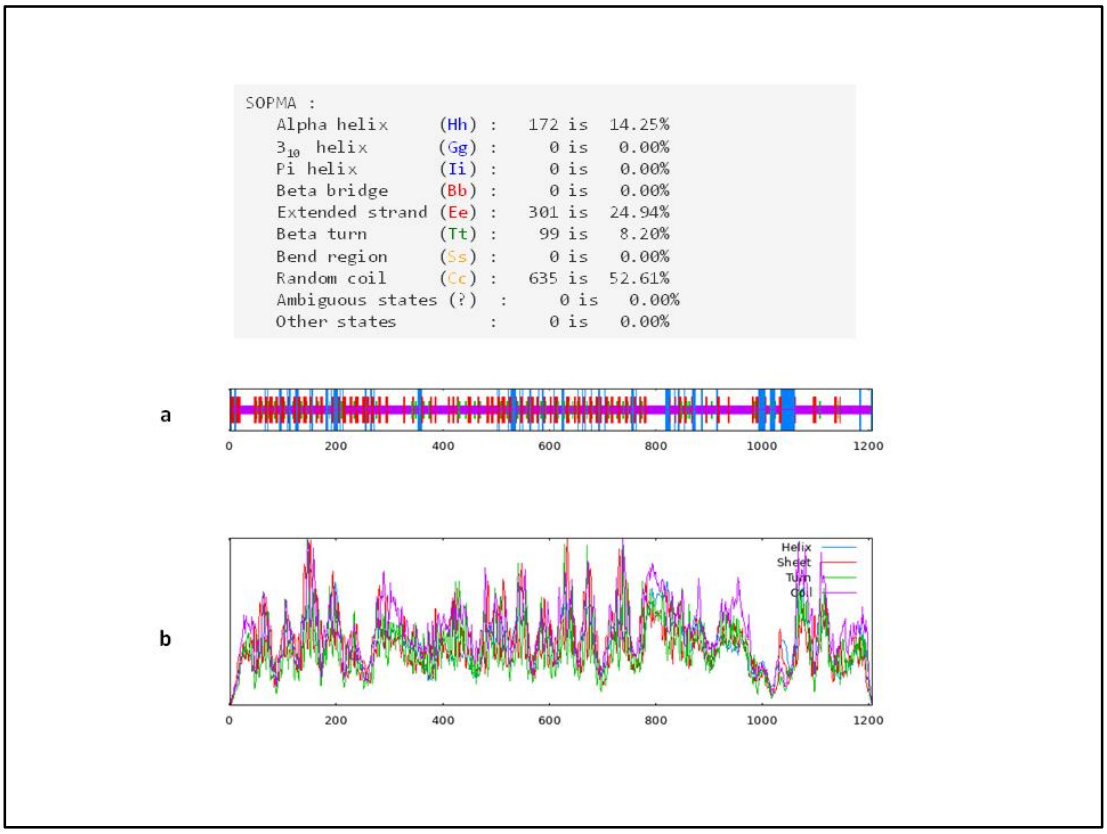

Fig.5: Secondary structure prediction of EGF using SOPMA. **(a)** Visualization of the predicted secondary structure elements (b) Score curves for each predicted state

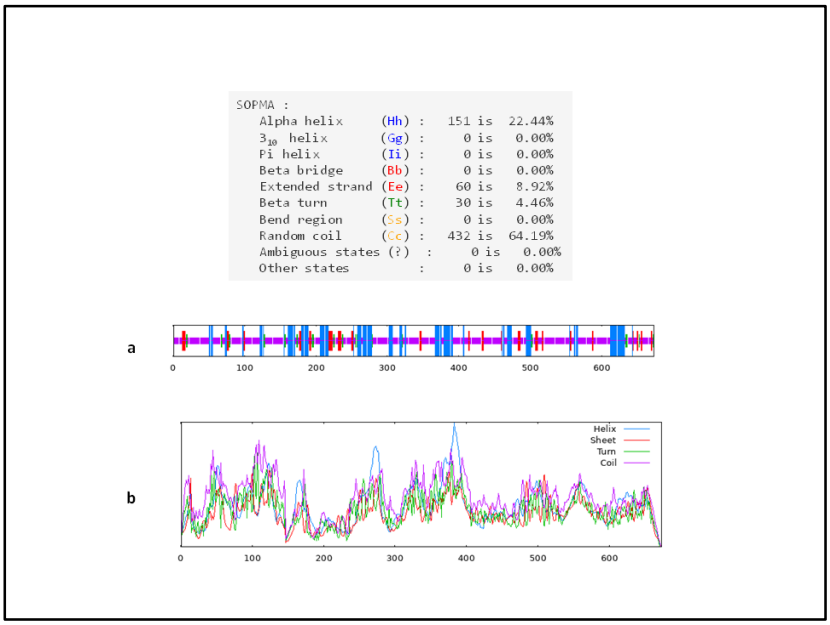

Fig.6: Secondary structure prediction of FOXO3 using SOPMA. **(a)** Visualization of the predicted secondary structure elements **(b)** Score curves for each predicted state

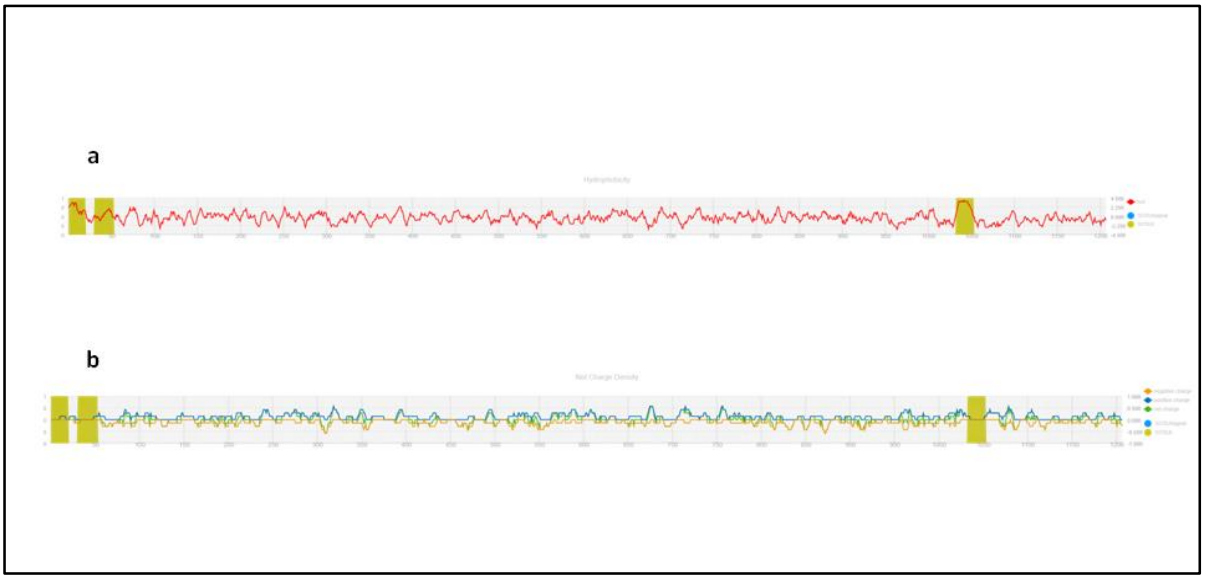

Fig.7: SOSUI secondary structure prediction of EGF. **(a)** Hydropathy plot showing hydrophobicity, with red indicating hydrophobic regions. **(b)** Charge plot, illustrating positively charged regions with blue and negatively charged regions with yellow.

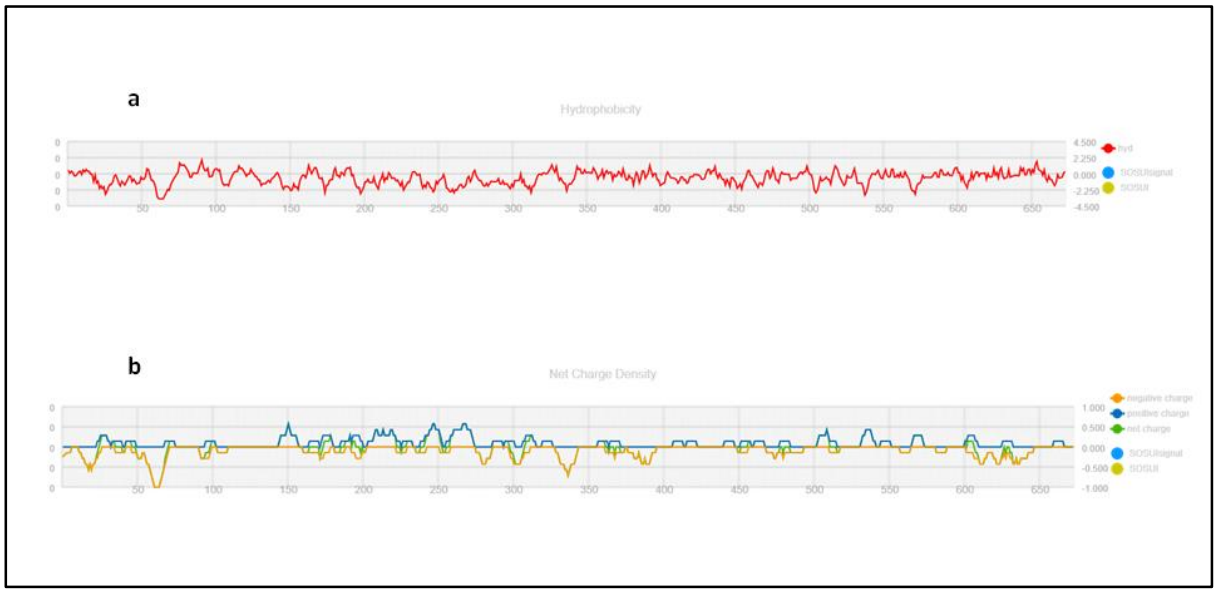

Fig.8: SOSUI secondary structure prediction of FOXO3. (a) Hydropathy plot showing hydrophobicity, with red indicating hydrophobic regions (b) Charge plot, illustrating positively charged regions with blue and negatively charged regions with yellow.

The three-dimensional (3D) structure of the proteins was modeled using SWISS-MODEL via homology modeling. Protein structure validation was carried out using PROCHECK UCLA, and the Ramachandran plot analysis revealed that 79.3% of EGF residues were within favored regions, with 3.0% in generously allowed regions and 2.9% in disallowed regions. Similarly, for FOXO3,

78.3% of residues were in favored regions, 3.6% in generously allowed regions, and 2.4% in disallowed regions, as illustrated in Figure 9.

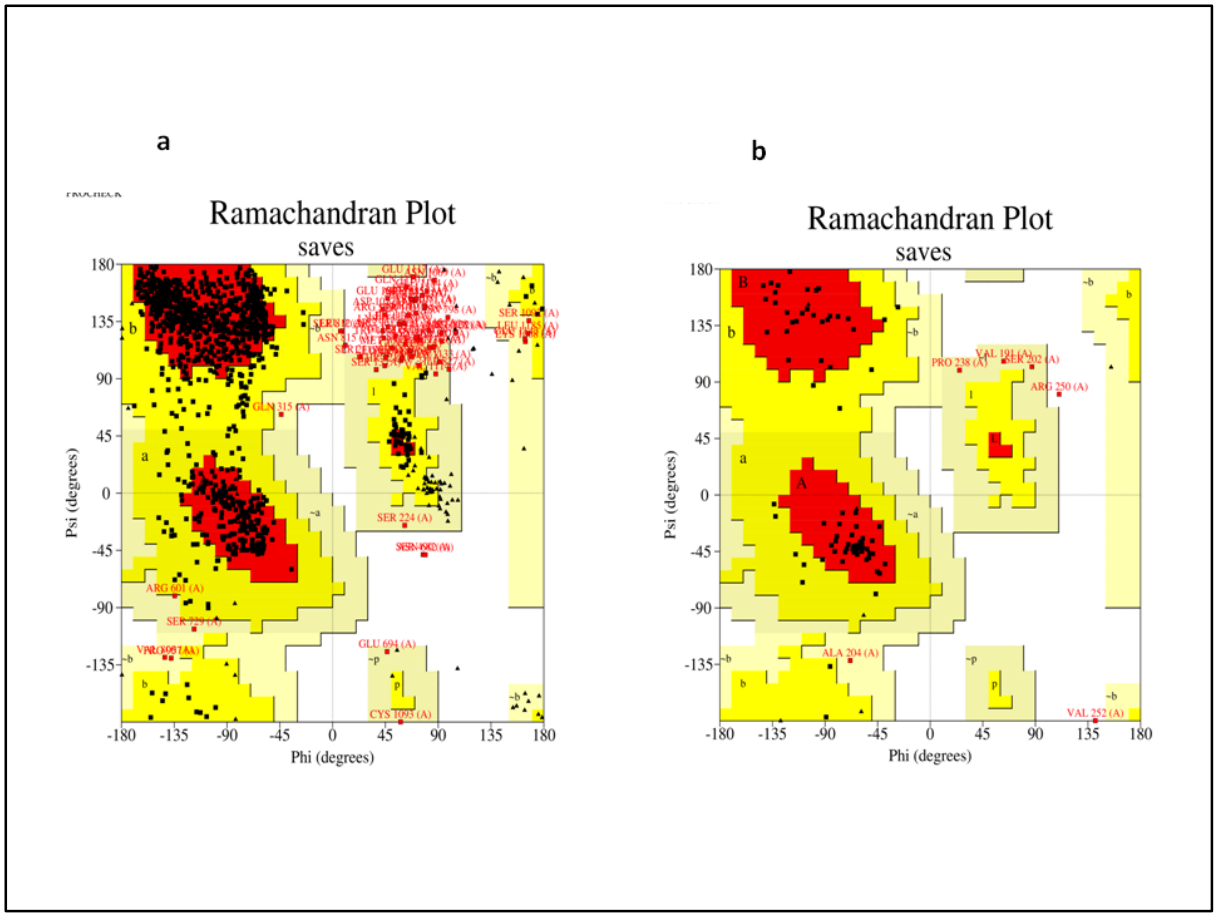

Fig.9: Ramachandran plot for (a) EGF (B) FOXO3

The receptors (EGF and FOXO3) were further refined using Chimera, where additional chains, ions, ligands, and solvent molecules were removed. Swiss PDB Viewer was employed for energy minimization of the receptors. Finally, Chimera was used for the final receptor preparation, which included the addition of hydrogens and charges, making the receptors ready for docking.

Table.2: Drug-likeness descriptors of 20 compounds calculated using DruLito software

Sr. No.	Title	MW	logp	Alogp	HBA	HBD	TPSA	AMR	Nrb	nAtom	nAcidicGroup	RC	nRigidB	nAromRing	nHB	SAlerts
1	5281810	462.12	-0.023	-2.977	11	6	175.37	118.26	5	55	0	4	31	2	17	1
2	5281607	254.06	1.852	0.339	4	2	66.76	78.55	1	29	0	3	20	2	6	1
3	1.02E+08	474.12	0.416	-2.292	11	5	164.37	120.43	5	56	1	5	33	3	16	1
4	107935	394.14	2.341	0.035	6	0	63.22	115.54	2	51	0	5	31	2	6	0
5	5377565	432.18	1.587	1.404	8	1	116.2	110.38	7	59	1	3	26	0	9	4
6	451674	552.31	7.052	0.99	7	3	129.51	145.51	4	86	2	5	38	0	10	2
7	16590	146.02	2.266	2.619	0	0	50.6	45.31	5	18	0	0	2	0	0	3
8	16315	177.99	2.521	3.21	0	0	75.9	53.1	6	19	0	0	2	0	0	3
9	10281	164.08	1.102	1.018	2	0	34.14	48.51	1	24	0	1	11	0	2	1
10	159134	844.24	1.672	-1.783	20	5	278.8	199.69	17	104	0	6	48	2	25	4
11	253193	592.27	2.602	1.31	9	3	132.94	175.38	7	80	1	6	42	0	12	4
12	5280863	286.05	1.486	-0.681	6	4	107.22	81.83	1	31	0	3	22	2	10	1
13	1.63E+08	416.11	1.61	-1.571	9	2	112.91	112.84	5	50	0	4	28	2	11	2
14	1.68E+08	300.21	3.24	1.004	2	1	37.3	87.46	1	50	0	4	24	0	3	1
15	969516	368.13	1.945	0.522	6	2	93.06	111.7	8	47	0	2	20	2	8	2
16	82755	154.06	0.385	-0.112	3	3	60.69	44.68	2	21	0	1	9	1	6	1
17	162209	316.2	5.337	1.155	3	2	57.53	92.37	2	51	1	3	23	1	5	0
18	5281717	244.07	1.545	0.631	4	4	80.92	76.21	2	30	0	2	17	2	8	1
19	160254	296.14	3.114	0.661	3	0	43.37	86.33	0	42	0	4	25	1	3	2
20	68827	282.15	3.039	0.801	5	0	53.99	61.35	0	42	0	4	23	0	5	3

Toxicity analysis was conducted to evaluate the compounds for tumorigenicity, mutagenicity, irritant potential, and reproductive toxicity using the OSIRIS Property Explorer. Of the 20 selected ligands, 15 compounds met the drug-likeness criteria and passed toxicity screening, as shown in Table 3. The non-toxic compounds included Chrysin, Deguelin, Pseudolaric acid-B, Triterpenoid, Diallyl disulfide, Diallyl trisulfide, Scabraside, Pheophorbide a, Aleuritin, Aleuritone, Curcumin, Hydroxytyrosol, Pisiferic acid, Oxyresveratrol, and Cryptotanshinone. These 15 compounds were subsequently subjected to docking studies to evaluate their binding affinities and interactions with the target receptors.

Table.3: Toxicity profile of the 20 compounds

S.No.	Name	CID	cLOG P	SOLUBILITY	MOL WT	TPSA	DRUGLIKELINESS	DRUG SCORE	MUTAGENICITY	TUMORIGENICITY	IRRITANT	REPRODUCTIVE EFFECT
1	Tectoridin	5281810	-0.43	-2.63	462	175.3	-2.52	0.15	1	0.6	1	0.6
2	Chrysin	5281607	2.68	-3.15	254	66.76	0.97	0.75	1	1	1	1
3	8-methoxy-10-[(	101948691	1.24	-5.16	474	164.3	-3.75	0.1	0.6	0.6	1	1
4	Deguelin	107935	4.13	-5.2	394	63.22	0.4	0.26	1	1	1	0.6
5	Pseudolaric acid	5377565	2.14	-3.05	432	116.2	-2.03	0.43	1	1	1	1
6	Triterpenoid	451674	3.52	-4.48	552	129.5	-1.41	0.3	1	1	1	1
7	Diallyl disulfide	16590	2.93	-2.71	146	50.6	-4.7	0.45	1	1	1	1
8	Diallyl trisulfide	16315	2.33	-3.3	178	75.9	-4.7	0.45	1	1	1	1
9	Thymoquinone	10281	1.64	-1.68	164	34.14	-1.2	0.35	0.6	1	1	1
10	Scabraside	159134	0.49	-4.64	844	278.8	-5.27	0.2	1	1	1	1
11	Pheophorbide a	253193	4.17	-5.75	592	132.9	-3.18	0.18	1	1	1	1
12	Kaempferol	5280863	1.84	-2.79	286	107.2	0.9	0.46	0.6	1	1	1
13	Aleuritin	163097522	1.83	-3.28	416	112.9	-0.94	0.5	1	1	1	1
14	Aleuritone	168353583	3.67	-3.97	300	37.3	-3.78	0.38	1	1	1	1
15	Curcumin	969516	2.95	-3.62	368	93.06	-3.95	0.4	1	1	1	1
16	Hydroxytyrosol	82755	0.8	-1.02	154	60.69	-1.3	0.59	1	1	1	1
17	Pisiferic Acid	162209	4.09	-4.54	316	57.53	-6.69	0.33	1	1	1	1
18	Oxyresveratrol	5281717	2.48	-2.57	244	80.92	-3.59	0.28	1	1	1	0.6
19	Cryptotanshinon	160254	3.39	-4.49	296	43.37	-7.06	0.21	1	1	1	0.6
20	Artemisinin	68827	2.26	-3.29	282	53.99	-1.97	0.17	1	0.6	0.6	1

3.4. Docking Studies

Molecular docking was performed for the 15 screened compounds with the target receptors EGF and FOXO3. The binding pocket coordinates for EGF, obtained from CASTp, were -15.646, 22.390, 2.681, and for FOXO3, they were 6.299, -19.954, -1.830. The pocket center size was set to 20 for all three dimensions. Docking results were evaluated based on binding energies (ΔG). The best result for EGF was a binding energy of -6.5 kcal/mol with pheophorbide a, while for FOXO3, the best score was -6.9 kcal/mol with Curcumin. These two compounds were selected based on their low binding energies and high binding affinities, as shown in (Table 4). Additional docking scores and interactions are summarized in (Table 5). The binding energies indicate strong binding affinity and stability of these compounds with their respective target receptors.

Table 4: The two selected compounds with high binding affinity and their interactions 3.5

Compounds	Vina Score/Binding Affinity	Ligand	Distance (Å)	Target Protein	Category	Type Of Interaction
EGF-Pheophorbide a	-6.5	UNL1:C	4.88	A:ARG678	Hydrophobic	Alkyl Interaction
		UNL1	3.99	A:ARG678	Hydrophobic	Pi-Alkyl Interaction
		UNL1:H	2.31	UNL1:N	Hydrogen Bond	Conventional Hydrogen Bond Interaction
		UNL1:H	2.33	UNL1:N	Hydrogen Bond	Conventional Hydrogen Bond Interaction
		UNL1:C	4.74	A:ARG677	Hydrophobic	Alkyl Interaction
		UNL1:O	1.98	A:GLN681 :HN	Hydrogen Bond	Convention al Hydrogen Bond Interaction
		UNL1:H	2.46	A:ASP683: OD2	Hydrogen Bond	Conventional Hydrogen Bond Interaction
		UNL1:C	3.65	A:THR714: O	Hydrogen bond	Carbon Hydrogen Bond Interaction
		UNL1	2.77	A:ARG677: HG1	Weak non-covalent Bond	Pi-Sigma Interaction

		UNL1:C	4.37	A:ARG677	Hydrophobic	Alkyl Interaction
		UNL1:O	2.73	A:GLN681: O	Non-Covalent	Unfavorable Acceptor-Acceptor Interaction
		UNL1:C	4.4	A:ARG678	Hydrophobic	Alkyl Interaction
FOXO3-Curcumin	-6.9	UNL1	3.77	A:TYR162	Van der waals forces	Pi-Pi Stacked Interaction
		UNL1:C	5.19	A:TRP186	Hydrophobic	Pi-Alkyl Interaction
		UNL1	3.99	A:VAL191	Hydrophobic	Pi-Alkyl Interaction
		UNL1:O	2.95	A:ASN159: HN	Hydrogen Bond	Conventional Hydrogen Bond Interaction
		UNL1:O	2.59	A:GLY158: HT1	Hydrogen Bond	Conventional Hydrogen Bond Interaction
		UNL1:O	2.15	A:TYR162: HN	Hydrogen Bond	Conventional Hydrogen Bond Interaction
		UNL1:C	5.13	A:VAL191	Hydrophobic	Alkyl Interaction
		UNL1:O	2.43	A:LEU160: HN	Hydrogen Bond	Conventional Hydrogen Bond Interaction

Table 5: Docking scores and interactions of the 20 compounds with the target receptor is shown in table below

Compounds	**Vina Score/Binding Affinity**	**Ligand**	**Distance (Å)**	**Target Protein**	**Category**	**Type Of Interaction**
EGF-Chrysin	-5.3	UNL1	4.28	A:ARG633	Hydrophobic	Pi-Alkyl Interaction
		UNL1	4.41	A:ARG633	Hydrophobic	Pi-Alkyl Interaction
		UNL1	4.51	A:GLU595:OE2	Weak non-covalent Bond	Pi-Anion Interaction

		UNL1:O	2.2	A:GLU595:HN	Hydrogen Bond	Conventional Hydrogen Bond Interaction
		UNL1:O	2.03	A:LYS594:HN	Hydrogen Bond	Conventional Hydrogen Bond Interaction
		UNL1:O	2.5	A:THR593:HA	Hydrogen Bond	Carbon Hydrogen Bond Interaction
EGF- Deguelin	-5.9	UNL1:O	2.88	A:GLN681:HN	Hydrogen Bond	Conventional Hydrogen Bond Interaction
		UNL1:O	2.59	A:THR680:HA	Hydogen Bond	Carbon Hydrogen Bond Interaction
		UNL1:C	3.11	A:LEU679:O	Hydrogen Bond	Carbon Hydrogen Bond Interaction
		UNL1	4.89	A:ARG718	Hydrophobic	Alkyl Interaction
		UNL1	4.51	A:LYS716	Hydrophobic	Alkyl Interaction
		UNL1	2.55	A:LYS716:HG1	Weak non-covalent Bond	Pi-Sigma Interaction
		UNL1:O	2.82	A:ARG718:HH21	Hydrogen Bond	Conventional Hydrogen Bond Interaction
		UNL1:O	2.33	A:ARG718:HH22	Hydrogen Bond	Conventional Hydrogen Bond Interaction
EGF- Pseudolaric acid-B	-5.5	UNL1:C	3.76	A:ARG678	Hydrophobic	Alkyl Interaction
		UNL1	4.76	A:LYS716	Hydrophobic	Alkyl Interaction
		UNL1:O	2.41	A:LYS716:HA	Hydrogen bond	Carbon Hydrogen Bond Interaction
		UNL1:H	2.49	A:GLY715:O	Hydrogen Bond	Conventional Hydrogen Bond Interaction
		UNL1:H	1.27	A:ARG718:HH22	Non-Covalent	Unfavorable Donor-Donor Interaction
		UNL1:C	4.31	A:LYS716	Hydrophobic	Alkyl Interaction
EGF- Triterpenoid	-6.3	UNL1:C	4.18	A:ARG678	Hydrophobic	Alkyl Interaction
		UNL1:O	2.77	A: GLN681:O	Non-Covalent	Unfavorable Acceptor-

						Acceptor Interaction
		UNL1:H	2.39	A:GLN681:OE1	Hydrogen Bond	Conventional Hydrogen Bond Interaction
		UNL1:O	2.2	A:GLN681:HN	Hydrogen Bond	Conventional Hydrogen Bond Interaction
		UNL1:C	4.16	A:PRO442	Hydrophobic	Alkyl Interaction
		UNL1	4.99	A:PRO442	Hydrophobic	Alkyl Interaction
EGF-Diallyl disulfide	-2.7	UNL1:C	4.83	A:MET668	Hydrophobic	Alkyl Interaction
		UNL1	4.9	A:ARG713	Hydrophobic	Alkyl Interaction
		UNL1	5.07	A:ARG713	Hydrophobic	Alkyl Interaction
		UNL1:C	4.13	A:ARG713	Hydrophobic	Alkyl Interaction
		UNL1:C	3.73	A:LYS712	Hydrophobic	Alkyl Interaction
EGF-Diallyl trisulfide	-2.6	UNL1:C	4.6	A:LYS655	Hydrophobic	Alkyl Interaction
		UNL1:C	4.54	A:LYS712	Hydrophobic	Alkyl Interaction
		UNL1:C	4.62	A:MET668	Hydrophobic	Alkyl Interaction
		UNL1	5.16	A:MET668	Hydrophobic	Alkyl Interaction
		UNL1	4.3	A:ARG713	Hydrophobic	Alkyl Interaction
		UNL1:S	3.08	A:ARG677:NH1	Non- covalent	Sulfur-X Interaction
		UNL1:C	4.16	A:LYS675	Hydrophobic	Alkyl Interaction
		UNL1	4.48	A:LYS712	Hydrophobic	Alkyl Interaction
EGF-Scabraside	-5.6	UNL1:O	2.33	A:GLN681:HN	Hydrogen Bond	Conventional Hydrogen Bond Interaction
		UNL1:C	3.41	A:ASP683:OD2	Hydrogen Bond	Carbon Hydrogen Bond Interaction
		UNL1	3.73	UNL1	Van der waals forces	Pi-Pi Stacked Interaction

		UNL1	4.34	UNL1		Pi-Pi Stacked Interaction
		UNL1	4.33	A:LYS716	Hydrophobic	Pi-Alkyl Interaction
		UNL1:H	2.79	UNL1:O	Hydrogen Bond	Conventional Hydrogen Bond Interaction
		UNL1:O	2.92	A:THR680:HA	Hydrogen bond	Carbon Hydrogen Bond Interaction
		UNL1:H	2.79	A:LEU679:O	Hydrogen Bond	Conventional Hydrogen Bond Interaction
		UNL1	5.54	A:MET668	Non-covalent	Pi-Sulfur Interaction
		UNL1:O	2.71	A:ARG677:HH11	Hydrogen Bond	Conventional Hydrogen Bond Interaction
		UNL1:H	2.54	A:THR714:O	Hydrogen Bond	Conventional Hydrogen Bond Interaction
		UNL1:H	2.53	A:ARG678:O	Hydrogen Bond	Conventional Hydrogen Bond Interaction
		UNL1:O	3.1	A:LYS716:HE2	Hydrogen bond	Carbon Hydrogen Bond Interaction
		UNL1:H	2.56	UNL1:O	Hydrogen Bond	Conventional Hydrogen Bond Interaction
		UNL1:H	2.45	A:THR714:O	Hydrogen Bond	Conventional Hydrogen Bond Interaction
EGF-Pheophorbide a	-6.5	UNL1:C	4.88	A:ARG678	Hydrophobic	Alkyl Interaction
		UNL1	3.99	A:ARG678	Hydrophobic	Pi-Alkyl Interaction
		UNL1:H	2.31	UNL1:N	Hydrogen Bond	Conventional Hydrogen Bond Interaction
		UNL1:H	2.33	UNL1:N	Hydrogen Bond	Conventional Hydrogen Bond Interaction
		UNL1:C	4.74	A:ARG677	Hydrophobic	Alkyl Interaction
		UNL1:O	1.98	A:GLN681:HN	Hydrogen Bond	Conventional Hydrogen Bond Interaction

		UNL1:H	2.46	A:ASP683:OD2	Hydrogen Bond	Conventional Hydrogen Bond Interaction
		UNL1:C	3.65	A:THR714:O	Hydrogen bond	Carbon Hydrogen Bond Interaction
		UNL1	2.77	A:ARG677:HG1	Weak non-covalent Bond	Pi-Sigma Interaction
		UNL1:C	4.37	A:ARG677	Hydrophobic	Alkyl Interaction
		UNL1:O	2.73	A:GLN681:O	Non-Covalent	Unfavorable Acceptor-Acceptor Interaction
		UNL1:C	4.4	A:ARG678	Hydrophobic	Alkyl Interaction
EGF-Aleuritin	-6	UNL1:C	3.31	A:THR714:O	Hydrogen bond	Carbon Hydrogen Bond Interaction
		UNL1:C	3.77	A:THR7184:O	Hydrogen bond	Carbon Hydrogen Bond Interaction
		UNL1:H	2.34	A:GLY715:O	Hydrogen Bond	Conventional Hydrogen Bond Interaction
		UNL1:H	2.51	A:ARG713:O	Hydrogen Bond	Conventional Hydrogen Bond Interaction
		UNL1:C	4.83	A:LEU679:O	Hydrophobic	Alkyl Interaction
		UNL1:C	3.58	A:ARG678:O	Hydrogen bond	Carbon Hydrogen Bond Interaction
		UNL1:O	2.63	A:THR680:HA	Hydrogen bond	Carbon Hydrogen Bond Interaction
		UNL1:C	4.47	A:ARG677	Hydrophobic	Alkyl Interaction
EGF-Aleuritone	-5.3	UNL1:O	2.73	A:LYS716	Hydrogen bond	Carbon Hydrogen Bond Interaction
		UNL1:O	3.1	A:LYS716:HZ3	Hydrogen Bond	Conventional Hydrogen Bond Interaction
		UNL1:O	2.96	A:THR714:HB	Hydrogen bond	Carbon Hydrogen Bond Interaction
		UNL1:C	4.79	A:ARG713	Hydrophobic	Alkyl Interaction

		UNL1:C	3.88	A:PRO442	Hydrophobic	Alkyl Interaction
		UNL1:O	2.18	A:ARG677:HH11	Hydrogen Bond	Conventional Hydrogen Bond Interaction
		UNL1:C	4.71	A:ARG677	Hydrophobic	Alkyl Interaction
		UNL1:C	4.14	A:ARG677	Hydrophobic	Alkyl Interaction
EGF-Curcumin	-5.3	UNL1:C	3.65	A:ASP683:OD2	Hydrogen bond	Carbon Hydrogen Bond Interaction
		UNL1:O	2.59	A:ARG718:HH21	Hydrogen Bond	Conventional Hydrogen Bond Interaction
		UNL1:O	2.38	A:ARG718:HH22	Hydrogen Bond	Conventional Hydrogen Bond Interaction
		UNL1:O	2.23	A:GLN681:HN	Hydrogen Bond	Conventional Hydrogen Bond Interaction
		UNL1	5.18	A:ARG677	Hydrophobic	Pi-Alkyl Interaction
		UNL1:O	2.11	A:ARG678:HN	Hydrogen Bond	Conventional Hydrogen Bond Interaction
EGF-Hydroxytyrosol	-4.6	UNL1:O	2.42	A:ARG677:HH12	Hydrogen Bond	Conventional Hydrogen Bond Interaction
		UNL1:H	1.98	A:PRO442:O	Hydrogen Bond	Conventional Hydrogen Bond Interaction
		UNL1	4.16	A:ARG713:NH2	Non-covalent	Pi-Cation
		UNL1	4.64	A:ARG713	Hydrophobic	Pi-Alkyl Interaction
		UNL1:H	2.08	A:ARG713:O	Hydrogen Bond	Conventional Hydrogen Bond Interaction
		UNL1:H	1.33	A:LYS655:HZ3	Hydrogen bond donor	Unfavorable Donor-Donor Interaction
EGF-Pisiferic acid	-5.3	UNL1:O	2.64	A:LEU679:HA	Hydrogen bond	Carbon Hydrogen Bond Interaction
		UNL1:H	1.97	A:LEU679:O	Hydrogen Bond	Conventional Hydrogen Bond Interaction

		UNL1:O	2.2	A:ARG718:HH22	Hydrogen Bond	Conventional Hydrogen Bond Interaction
EGF-Oxyresveratrol	-5.1	UNL1	5.17	A:MET668:SD	Non-covalent	Pi-Sulfur Interaction
		UNL1	4.86	A:LYS655:NZ	Non-covalent	Pi-Cation Interaction
		UNL1	4.9	A:ARG677	Hydrophobic	Pi-Alkyl Interaction
		UNL1:O	2.86	A:ARG713:HH21	Hydrogen Bond	Conventional Hydrogen Bond Interaction
		UNL1	5.25	A:LYS712	Hydrophobic	Pi-Alkyl Interaction
		UNL1	4.9	A:ARG677	Hydrophobic	Pi-Alkyl Interaction
		UNL1	4.42	A:ARG713	Hydrophobic	Pi-Alkyl Interaction
		UNL1	2.93	A:ARG677:HD2	Weak non-covalent Bond	Pi-Sigma Interaction
		UNL1	3.84	A:ARG677:NH1	Non-covalent	Pi-Cation; Pi-Donor Hydrogen Bond Interaction
		UNL1	4.41	A:ARG713:NH1	Non-covalent	Pi-Cation Interaction
EGF-Cryptotanshinone	-5.9	UNL1	5.22	A:PRO465	Hydrophobic	Alkyl Interaction
		UNL1	5.26	A:TRP764	Van der waals forces	Pi-Pi Stacked Interaction
		UNL1	4.46	A:TRP674	Van der waals forces	Pi-Pi Stacked Interaction
		UNL1	5.53	A:TRP764	Van der waals forces	Pi-Pi Stacked Interaction
FOXO3-Chrysin	-6.5	UNL1:O	2.9	A:GLY158:HT2	Hydrogen Bond	Conventional Hydrogen Bond Interaction
		UNL1:O	2.06	A:GLY158:HT1	Hydrogen Bond	Conventional Hydrogen Bond Interaction
		UNL1	4.2	A:TYR193	Van der waals forces	Pi-Pi Stacked Interaction
		UNL1	3.88	A:TYR193	Van der waals forces	Pi-Pi Stacked Interaction
		UNL1	5.5	A:VAL191	Hydrophobic	Pi-Alkyl Interaction
		UNL1	3.72	A:TYR162	Van der waals	Pi-Pi Stacked

					forces	Interaction
		UNL1:H	1.92	UNL1:O	Hydrogen Bond	Conventional Hydrogen Bond Interaction
FOXO3- Deguelin	-5.7	UNL1:C	4.36	A:VAL191	Hydrophobic	Alkyl Interaction
		UNL1:C	4.38	A:TYR193	Hydrophobic	Pi-Alkyl Interaction
		UNL1	4.03	A:TYR193	Hydrophobic	Pi-Alkyl Interaction
		UNL1	5.27	A:TYR193		Pi-Pi Stacked Interaction
		UNL1:O	2.88	A:TYR193:HH	Hydrogen Bond	Conventional Hydrogen Bond Interaction
		UNL1	4.65	A:TYR162	Van der waals forces	Pi-Pi Stacked Interaction
		UNL1:C	5.09	A:TYR162	Hydrophobic	Pi-Alkyl Interaction
		UNL1:C	3.53	A:SER209:OG	Hydrogen Bond	Carbon Hydrogen Bond Interaction
		UNL1:C	4.92	A:LEU165	Hydrophobic	Alkyl Interaction
		UNL1:C	4.42	A:LEU160	Hydrophobic	Alkyl Interaction
		UNL1	4.65	A:TYR162	Van der waals forces	Pi-Pi Stacked Interaction
		UNL1	3.26	A:TYR162:HH	Non-covalent	Pi-Donor Hydrogen Bond Interaction
FOXO3- Pseudolaric acid-B	-5.4	UNL1:C	4.68	A:VAL191	Hydrophobic	Alkyl Interaction
		UNL1:O	2.16	A:GLY158:HT3	Hydrogen Bond	Conventional Hydrogen Bond Interaction
		UNL1	3.69	A:TYR193	Hydrophobic	Pi-Alkyl Interaction
		UNL1:C	4.29	A:TYR193	Hydrophobic	Pi-Alkyl Interaction
		UNL1	5.2	A:TYR193	Hydrophobic	Pi-Alkyl Interaction
		UNL1:O	2.99	A:LEU160:O	Non-Covalent	Unfavorable Acceptor-Acceptor Interaction
		UNL1:O	2.57	A:SER161:H	Hydrogen	Carbon Hydrogen Bond

				A	bond	Interaction
		UNL1	4.78	A:TYR162	Hydrophobic	Pi-Alkyl Interaction
		UNL1:C	4.06	A:TYR162	Hydrophobic	Pi-Alkyl Interaction
		UNL1:O	2.57	A:SER161:HA	Hydrogen bond	Carbon Hydrogen Bond Interaction
		UNL1:O	2.51	A:TYR162:HN	Hydrogen Bond	Conventional Hydrogen Bond Interaction
		UNL1:C	3.61	A:ASN213:OD1	Hydrogen bond	Carbon Hydrogen Bond Interaction
		UNL1:O	2.03	A:TYR162:HH	Hydrogen bond	Conventional Hydrogen Bond Interaction
FOXO3-Triterpenoid	-4	UNL1:C	4.85	A:TRP186	Hydrophobic	Pi-Alkyl Interaction
		UNL1:C	5.49	A:TRP186	Hydrophobic	Pi-Alkyl Interaction
		UNL1:C	3.46	A:VAL191	Hydrophobic	Alkyl Interaction
		UNL1	4.58	A:VAL191	Hydrophobic	Alkyl Interaction
		UNL1	3.89	A:VAL191	Hydrophobic	Alkyl Interaction
		UNL1	4.1	A:VAL191	Hydrophobic	Alkyl Interaction
		UNL1:O	2.23	A:GLY158:HT1	Hydrogen Bond	Conventional Hydrogen Bond Interaction
		UNL1	5.44	A:LEU160	Hydrophobic	Alkyl Interaction
		UNL1:O	2.11	A:ARG168:HH22	Hydrogen Bond	Conventional Hydrogen Bond Interaction
		UNL1:C	4.72	A:ARG168	Hydrophobic	Alkyl Interaction
FOXO3-Diallyl disulfide	-3	UNL1	5.02	A:LEU160	Hydrophobic	Alkyl Interaction
		UNL1	4.35	A:LEU165	Hydrophobic	Alkyl Interaction
		UNL1	4.15	A:VAL191	Hydrophobic	Alkyl Interaction
		UNL1:C	3.73	A:VAL191	Hydrophobic	Alkyl Interaction

		UNL1	4.35	A:LEU165	Hydrophobic	Alkyl Interaction
		UNL1:C	4.14	A:LEU165	Hydrophobic	Alkyl Interaction
		UNL1:C	5.17	A:TYR193	Hydrophobic	Pi-Alkyl Interaction
		UNL1:C	4.45	A:TYR162	Hydrophobic	Pi-Alkyl Interaction
		UNL1:C	5.2	A:TYR193	Hydrophobic	Pi-Alkyl Interaction
		UNL1	5.45	A:TYR193	Hydrophobic	Pi-Alkyl Interaction
		UNL1:C	4.72	A:PHE194	Hydrophobic	Pi-Alkyl Interaction
		UNL1	3.97	A:TYR193	Hydrophobic	Pi-Alkyl Interaction
FOXO3-Diallyl trisulfide	-3.3	UNL1:C	4.27	A:LEU165	Hydrophobic	Alkyl Interaction
		UNL1	4.98	A:LEU165	Hydrophobic	Alkyl Interaction
		UNL1:C	4.95	A:PHE194	Hydrophobic	Pi-Alkyl Interaction
		UNL1:C	4.68	A:TYR193	Hydrophobic	Pi-Alkyl Interaction
		UNL1	4.37	A:TYR193	Hydrophobic	Pi-Alkyl Interaction
		UNL1	5.04	A:TYR162	Hydrophobic	Pi-Alkyl Interaction
		UNL1:C	3.56	A:TYR162	Hydrophobic	Pi-Alkyl Interaction
		UNL1:C	4.05	A:VAL191	Hydrophobic	Alkyl Interaction
		UNL1:S	3.95	A:TYR193	Non-covalent	Pi-Sulfur Interaction
		UNL1	5.29	A:VAL191	Hydrophobic	Alkyl Interaction
FOXO3-Scabraside	-4.2	UNL1:O	2.64	A:ARG168:HH12	Hydrogen bond	Conventional Hydrogen Bond Interaction
		UNL1:O	2.73	A:ARG168:HH22	Hydrogen bond	Conventional Hydrogen Bond Interaction
		UNL1	4.96	A:VAL191	Hydrophobic	Pi-Alkyl Interaction
		UNL1	5.13	A:PRO192	Hydrophobic	Pi-Alkyl

						Interaction
		UNL1:C	4.88	A:PRO192	Hydrophobic	Alkyl Interaction
		UNL1	4.98	UNL1	Van der waals forces	Pi-Pi Stacked Interaction
		UNL1:O	3	A:GLY158:HA1	Hydrogen bond	Carbon Hydrogen Bond Interaction
		UNL1:O	2.22	A:GLY158:HT3	Hydrogen bond	Conventional Hydrogen Bond Interaction
		UNL1	5.46	A:TYR162	Van der waals forces	Pi-Pi Stacked Interaction
		UNL1:H	2.84	UNL1:O	Hydrogen bond	Conventional Hydrogen Bond Interaction
		UNL1:C	4.76	A:TYR193	Hydrophobic	Pi-Alkyl Interaction
		UNL1:C	4.32	A:VAL191	Hydrophobic	Alkyl Interaction
		UNL1:O	2.5	A:GLY158:HT2	Hydrogen Bond	Conventional Hydrogen Bond Interaction
		UNL1:O	2.34	A:TYR162:HH	Hydrogen Bond	Conventional Hydrogen Bond Interaction
FOXO3-Pheophorbide a	-5.6	UNL1	5.38	A:PRO192	Hydrophobic	Alkyl Interaction
		UNL1:H	2.31	UNL1:N	Hydrogen Bond	Conventional Hydrogen Bond Interaction
		UNL1:O	2.22	A:VAL191:HN	Hydrogen Bond	Conventional Hydrogen Bond Interaction
		UNL1	4.25	A:PRO192	Hydrophobic	Pi-Alkyl Interaction
		UNL1:H	2.33	UNL1:N	Hydrogen Bond	Conventional Hydrogen Bond Interaction
		UNL1:C	4.4	A:LYS195	Hydrophobic	Alkyl Interaction
		UNL1:O	3.01	A:ARG189:HE	Hydrogen Bond	Conventional Hydrogen Bond Interaction
		UNL1:C	3.98	A:LYS195	Hydrophobic	Alkyl Interaction
		UNL1	5.23	A:PRO192	Hydrophobic	Pi-Alkyl Interaction

		UNL1:C	4.39	A:PRO192	Hydrophobic	Alkyl Interaction
FOXO3- Aleuritin	-5.4	UNL1:C	4.81	A:TYR162	Hydrophobic	Pi-Alkyl Interaction
		UNL1:C	4.47	A:TYR193	Hydrophobic	Pi-Alkyl Interaction
		UNL1	4.06	A:TYR193	Van der waals forces	Pi-Pi Stacked Interaction
		UNL1	3.97	A:TYR193	Van der waals forces	Pi-Pi Stacked Interaction
		UNL1	3.88	A:TYR162	Van der waals forces	Pi-Pi Stacked Interaction
		UNL1:C	5.11	A:TYR162	Hydrophobic	Pi-Alkyl Interaction
		UNL1:O	2.27	A:TYR162:HN	Hydrogen Bond	Conventional Hydrogen Bond Interaction
		UNL1:C	3.55	A:SER209:OG	Hydrogen bond	Carbon Hydrogen Bond Interaction
		UNL1:C	5.05	A:PHE194	Hydrophobic	Pi-Alkyl Interaction
		UNL1:C	4.42	A:LEU165	Hydrophobic	Alkyl Interaction
		UNL1:O	2.62	A:GLY158:HT2	Hydrogen Bond	Conventional Hydrogen Bond Interaction
		UNL1:O	2.75	A:GLY158:HT1	Hydrogen Bond	Conventional Hydrogen Bond Interaction
FOXO3- Aleuritone	-5.6	UNL1:C	4.6	A:TRP186	Hydrophobic	Pi-Alkyl Interaction
		UNL1:C	4.87	A:LEU178	Hydrophobic	Alkyl Interaction
		UNL1	5.49	A:LEU178	Hydrophobic	Alkyl Interaction
		UNL1:C	4.6	A:TRP186	Hydrophobic	Pi-Alkyl Interaction
		UNL1:C	4.15	A:ARG189	Hydrophobic	Alkyl Interaction
		UNL1:C	4.59	A:PRO174	Hydrophobic	Alkyl Interaction
		UNL1:O	2.57	A:PRO174:HD2	Hydrogen bond	Carbon Hydrogen Bond Interaction
FOXO3- Curcumin	-6.9	UNL1	3.77	A:TYR162	Van der waals forces	Pi-Pi Stacked Interaction

		UNL1:C	5.19	A:TRP186	Hydrophobic	Pi-Alkyl Interaction
		UNL1	3.99	A:VAL191	Hydrophobic	Pi-Alkyl Interaction
		UNL1:O	2.95	A:ASN159:HN	Hydrogen Bond	Conventional Hydrogen Bond Interaction
		UNL1:O	2.59	A:GLY158:HT1	Hydrogen Bond	Conventional Hydrogen Bond Interaction
		UNL1:O	2.15	A:TYR162:HN	Hydrogen Bond	Conventional Hydrogen Bond Interaction
		UNL1:C	5.13	A:VAL191	Hydrophobic	Alkyl Interaction
		UNL1:O	2.43	A:LEU160:HN	Hydrogen Bond	Conventional Hydrogen Bond Interaction
FOXO3-Hydroxytyrosol	-5.4	UNL1	4.61	A:LEU165	Hydrophobic	Pi-Alkyl Interaction
		UNL1	4.79	A:LEU160	Hydrophobic	Pi-Alkyl Interaction
		UNL1:O	2.76	A:ASN159:HN	Hydrogen Bond	Conventional Hydrogen Bond Interaction
		UNL1:H	2.69	A:LEU160:O	Hydrogen Bond	Conventional Hydrogen Bond Interaction
		UNL1	4.65	A:VAL191	Hydrophobic	Pi-Alkyl Interaction
		UNL1:H	2.36	A:CYS190:O	Hydrogen Bond	Conventional Hydrogen Bond Interaction
		UNL1:O	3.07	A:GLY158:HT2	Hydrogen Bond	Conventional Hydrogen Bond Interaction
FOXO3- Pisiferic acid	-6.2	UNL1:C	4.6	A:TYR162	Hydrophobic	Pi-Alkyl Interaction
		UNL1	4.39	A:TYR162	Hydrophobic	Pi-Alkyl Interaction
		UNL1	5.95	A:TYR162	Van der waals forces	Pi-Pi Stacked Interaction
		UNL1	4.22	A:TYR193	Van der waals forces	Pi-Pi Stacked Interaction
		UNL1:C	4.62	A:TYR193	Hydrophobic	Pi-Alkyl Interaction
		UNL1:O	2.17	A:TYR162:HH	Hydrogen Bond	Conventional Hydrogen Bond

						Interaction
		UNL1:H	1.39	A:TYR193:HH	Non-covalent	Unfavorable Donor-Donor Interaction
FOXO3-Oxyresveratrol	-5.7	UNL1:O	2.71	A:TYR162:HH	Hydrogen Bond	Conventional Hydrogen Bond Interaction
		UNL1	4.05	A:TYR193	Van der waals forces	Pi-Pi Stacked Interaction
		UNL1	3.64	A:TYR162	Van der waals forces	Pi-Pi Stacked Interaction
FOXO3-Cryptotanshinone	-6.1	UNL1	4.03	A:TYR193	Hydrophobic	Pi-Alkyl Interaction
		UNL1:C	3.82	A:VAL191	Hydrophobic	Alkyl Interaction
		UNL1:C	4.57	A:TYR193	Hydrophobic	Pi-Alkyl Interaction
		UNL1:C	3.82	A:VAL191	Hydrophobic	Alkyl Interaction
		UNL1:C	4.88	A:VAL191	Hydrophobic	Alkyl Interaction
		UNL1:C	4.37	A:LEU165	Hydrophobic	Alkyl Interaction
		UNL1;C	4.79	A:LEU165	Hydrophobic	Alkyl Interaction
		UNL1:C	3.87	A:LEU160	Hydrophobic	Alkyl Interaction
		UNL1	4.02	A:TYR193	Van der waals forces	Pi-Pi Stacked Interaction
		UNL1	4.36	A:TYR193	Van der waals forces	Pi-Pi Stacked Interaction

3.5. Visualization

The receptor-ligand interactions were visualized using Biovia Discovery Studio. The docked poses of the two compounds—Pheophorbide a with EGF and Curcumin with FOXO3—were examined and are depicted in Fig. 10 and Fig. 11, respectively.

In the interaction between EGF and Pheophorbide a, four conventional hydrogen bonds were observed. These bonds formed with UNL1 (at bond distances of 2.31 Å and 2.33 Å), GLN681 (1.98 Å), and ASP683 (2.46 Å). Additionally, one carbon hydrogen interaction was noted with THR174 at a bond distance of 3.65 Å. Several alkyl interactions were identified, including two with ARG678 (4.88 Å and 4.4 Å) and two with ARG677 (4.74 Å and 4.37 Å). A Pi-Alkyl interaction with ARG678 was observed at a bond distance of 3.99 Å, alongside a Pi-Sigma interaction with ARG677 at 2.77 Å. and one Unfavorable Acceptor-Acceptor Interaction with GLN681 having the bond distance of

2.73 Å.

In the interaction between FOXO3 and Curcumin, four conventional hydrogen bonds were formed with ASN159 (2.95 Å), GLY158 (2.59 Å), TYR162 (2.15 Å), and LEU160 (2.43 Å). Additionally, one Pi-Pi stacked interaction was identified with TYR162 at a bond distance of 3.77 Å. Two Pi-Alkyl interactions occurred with TRP186 and VAL191, at bond distances of 5.19 Å and 3.99 Å, respectively. An additional alkyl interaction was observed with VAL191 at a bond distance of 5.13 Å.

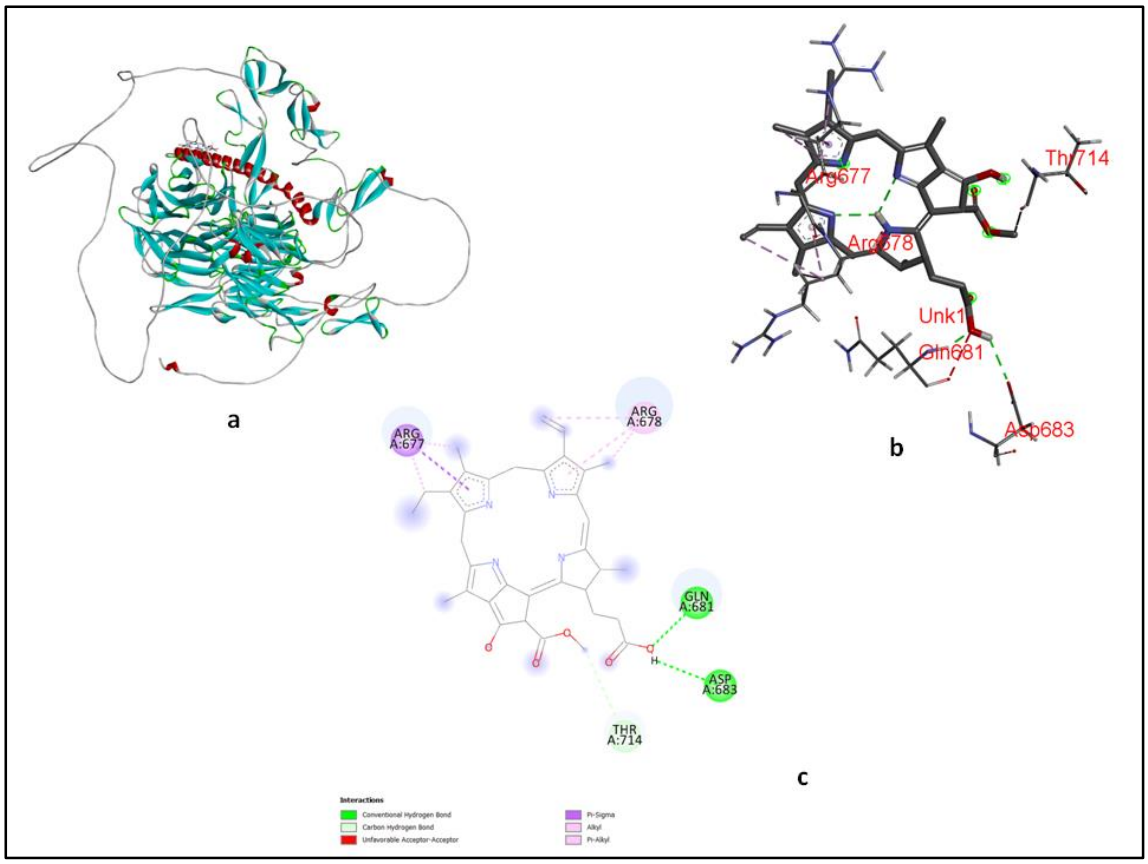

Fig.10:(a) Docked pose of the compound pheophorbide a with EGF receptor. **(b)** ligand interaction diagram showing important interactions involved in the complex as dashed lines. **(c)** 2D plot of the docked complex. All interactions were visualized or generated using Biovia Discovery Studio Visualizer.

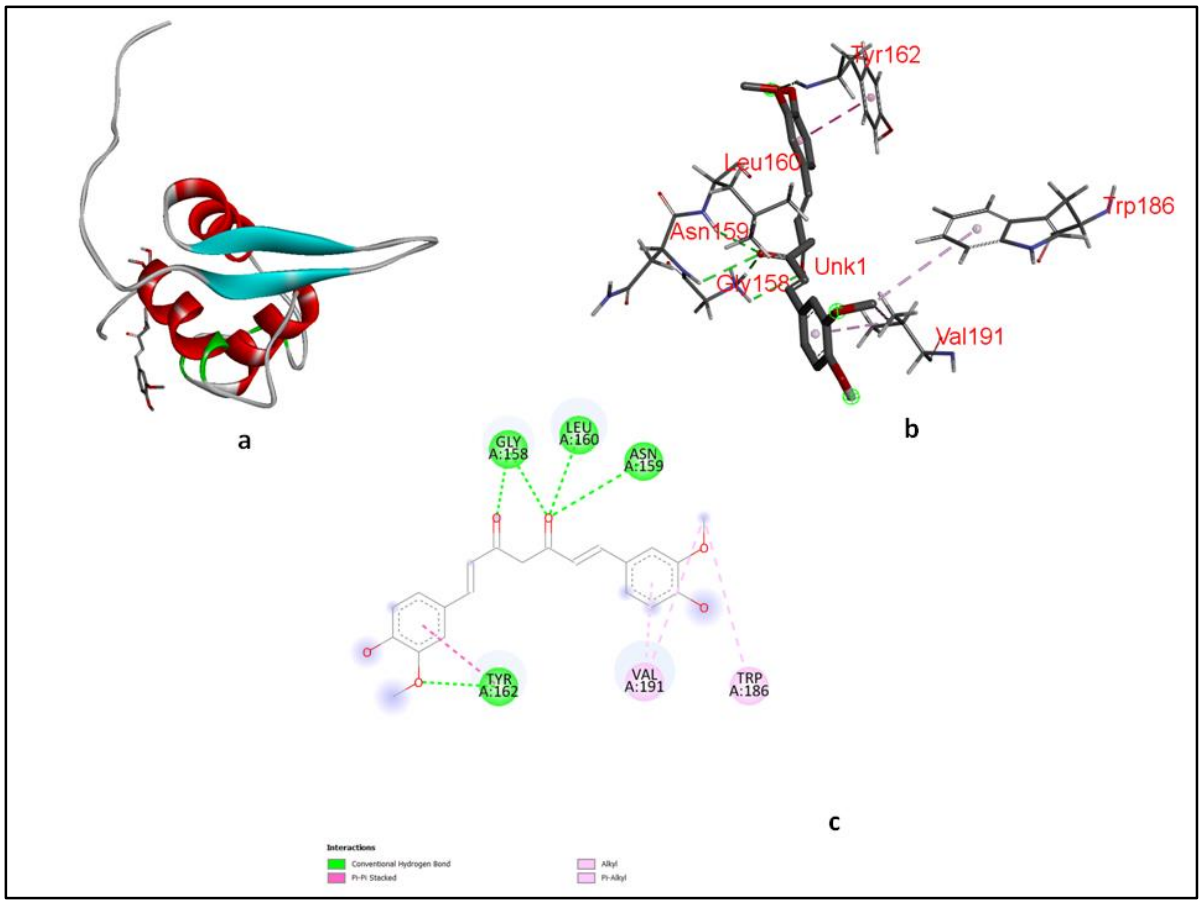

Fig.11: (a) Docked pose of the compound Curcumin with FOXO3 receptor. **(b)** ligand interaction diagram showing important interactions involved in the complex as dashed lines. **(c)** 2D plot of the docked complex. All interactions were visualized or generated using Biovia Discovery Studio Visualizer.

DISCUSSION

Sequencing data and bioinformatics approaches can identify novel targets, driver mutations, and dysregulated pathways in pancreatic cancer, potentially improving therapeutics, survival rates, and the quality of life for patients. In our study, we conducted a meta-analysis of five microarray gene expression profiling datasets, or case studies, related to pancreatic cancer. This analysis led to the identification of differentially expressed genes (DEGs) across various pancreatic cancer cases. Further gene conservancy analysis revealed a subset of significant DEGs common to all cases. Key hub genes, including EGF, PTEN, TGFB1, KRAS, CREBBP, PECAM1, FOXO3, H2BC21, FYN, and THBS1, were identified from the conserved gene set. These highly expressed genes may play critical roles in determining patient prognosis in pancreatic cancer. Variations in prognosis may stem from the regulatory functions of these genes. Among the identified DEGs, EGF and FOXO3 emerged as critical targets due to their involvement in tumor growth and survival pathways. EGF enhances cell growth and survival by activating pathways like the RAF-mitogen-activated protein kinase (MAPK) and phosphoinositide-3-kinase (PI3K) pathways [43]. EGFR, a glycoprotein and

tyrosine kinase receptor within the HER family, initiates signaling crucial for cell growth, differentiation, and survival [44]. EGFR is overexpressed in 30–95% of pancreatic cancer cases [45,46], with its overexpression linked to poor prognosis [47]. During the progression from pancreatic intraepithelial neoplasia (PanIN) to pancreatic ductal adenocarcinoma (PDAC), there is a notable increase in EGFR expression, marking a crucial molecular shift in pancreatic cancer development. In PDAC, tumor cells rely on both EGFR and K-Ras signaling for growth. While K-Ras oncogenes drive tumor proliferation, EGFR signaling is essential for initiating and advancing PDAC tumors. Targeting EGFR and its downstream pathways, such as PI3K and STAT3, could provide new therapeutic avenues. Notably, K-Ras alone does not activate key pathways like AKT and STAT3, but EGFR expression initiation cooperates with K-Ras to activate these signaling cascades in pancreatic lesions [48]. The combination of EGFR-targeted therapy with gemcitabine could potentially enhance pancreatic cancer outcomes [49]. While some combinations of EGFR inhibitors and chemotherapy show promise in inhibiting tumor growth and promoting cell death in animal models, their effectiveness still requires further validation. However, incorporating EGFR inhibition into a comprehensive treatment approach is emerging as a promising strategy for pancreatic cancer [45]. FOXO factors coordinate cellular responses by integrating various signals from inside and outside the cell, to balance growth-promoting cues with stress responses, determining whether cells grow, resist stress, or undergo apoptosis. FOXO3, a key member of this family (formerly known as FKHRL1), facilitates tumor progression and metastasis in pancreatic cancer by regulating cell proliferation, apoptosis, and DNA repair. Dysregulation of FOXO3 disrupts this balance, leading to uncontrolled cell growth and survival, thereby enhancing tumor aggressiveness [50]. In pancreatic cancer, FOXO3 facilitates tumor advancement and metastasis. A recent study revealed that cyclic GMP (cGMP) reduces CD44 expression and cancer stem cell (CSC) properties in pancreatic cancer by inhibiting FOXO3. High FOXO3 activation signatures in patients correlate with poor prognosis, highlighting the potential of targeting FOXO3 and cGMP as therapeutic strategies. Inhibiting FOXO3 disrupts CSC properties, potentially slowing tumor progression in PDAC [51]. A library of natural compounds targeting key receptors implicated in pancreatic cancer progression and metastasis, such as EGF and FOXO3, was created using data from scientific literature and the PubChem database. Compounds with known 3D structures were evaluated for drug-likeness and ADMET properties using DruLito, considering criteria such as molecular weight, logP, and hydrogen bonding potential. Further toxicity screening using OSIRIS ensured these compounds lacked tumorigenic, mutagenic, irritant, or reproductive toxicity properties. Molecular docking studies conducted with AutoDock Vina in UCSF Chimera identified pheophorbide a and curcumin as potential inhibitors of EGF and FOXO3, respectively. Pheophorbide a exhibited a binding energy of -6.5 kcal/mol with EGF, forming four conventional hydrogen bonds, one carbon hydrogen bond, and several hydrophobic interactions. Similarly,

curcumin showed a binding energy of -6.9 kcal/mol with FOXO3, forming four hydrogen bonds, a Pi-Pi stacked interaction, and multiple hydrophobic interactions. These interactions, as visualized using Biovia Discovery Studio, indicate that both compounds could inhibit the activity of their respective targets, potentially slowing pancreatic cancer progression. Studies have highlighted the ability of pheophorbide a to selectively induce cell death in cancer cells and reduce tumor size in vivo, emphasizing its potential as a therapeutic agent against this aggressive cancer type [52,53]. Similarly, curcumin's anti-cancer properties—such as inducing apoptosis, inhibiting cell proliferation, and enhancing sensitivity to chemotherapy—position it as a promising candidate for cancer therapy [54-57]. Targeted therapy connects tumor characterization with personalized treatment, using genomics and biomarkers to identify genetic mutations and pathway alterations as pharmacological targets or prognostic indicators. Advances in genome sequencing have enabled the rapid identification of genetic differences between tumor and normal cells [58]. Next-generation sequencing (NGS) has been particularly instrumental in identifying molecular alterations driving pancreatic cancer progression. Sequencing data have also revealed the highly heterogeneous nature of pancreatic tumors, which often exhibit resistance to traditional chemotherapy and radiation therapies [59]. This underscores the challenges in treating pancreatic cancer, highlighting the need for more personalized, targeted therapeutic strategies. This study highlights the importance of bioinformatics and computational biology in drug discovery, particularly for complex diseases like pancreatic cancer. By integrating gene expression profiling, molecular docking, and toxicity screening, we identified natural compounds with potential therapeutic efficacy. Our findings suggest that pheophorbide a and curcumin could be promising candidates for further preclinical and clinical evaluation, potentially offering new avenues for the treatment of pancreatic cancer.

4. CONCLUSION

Pancreatic cancer remains one of the most aggressive cancers, and current treatments are often ineffective, necessitating novel strategies. Our computational analysis identified key genes, EGF and FOXO3, which play crucial roles in pancreatic cancer progression. EGF and its receptor, EGFR, regulate cell proliferation and survival, while FOXO3, involved in apoptosis and cell cycle regulation, is often suppressed in cancer. Through bioinformatic approaches, including compound screening and docking studies, we identified pheophorbide a and curcumin as potential inhibitors of these targets. These findings highlight the promise of targeting EGF and FOXO3 with natural compounds for therapeutic strategies. Further experimental validation is needed to confirm these findings and explore their clinical potential. Future research should focus on in vitro and in vivo studies to advance these compounds as effective treatments.

ETHICS APPROVAL AND CONSENT TO PARTICIPATE

Not applicable.

HUMAN AND ANIMAL RIGHTS

No animals or humans were used for the studies that are based on this research.

CONSENT FOR PUBLICATION

Not applicable.

FUNDING

None.

ACKNOWLEDGEMENT

I would like to acknowledge Head,Departmentof Tech Biosciencesat Digianalix, for providing research facility, funding support and assistance for completion of project.

CONFLICT OF INTEREST

There was no conflict of interest.

REFERENCES

1. International Agency for Research on Cancer. Cancer incidence in five continents. (No Title). 2022 Jan 1.
2. Sung H, Ferlay J, Siegel RL, Laversanne M, Soerjomataram I, Jemal A, Bray F. Global cancer statistics 2020: GLOBOCAN estimates of incidence and mortality worldwide for 36 cancers in 185 countries. CA: a cancer journal for clinicians. 2021 May;71(3):209-49.
3. Rahib L, Smith BD, Aizenberg R, Rosenzweig AB, Fleshman JM, Matrisian LM. Projecting cancer incidence and deaths to 2030: the unexpected burden of thyroid, liver, and pancreas cancers in the United States. Cancer research. 2014 Jun 1;74(11):2913-21.
4. Carrato A, Falcone A, Ducreux M, Valle JW, Parnaby A, Djazouli K, et.al. A systematic review of the burden of pancreatic cancer in Europe: real-world impact on survival, quality of life and costs. Journal of gastrointestinal cancer. 2015 Sep;46:201-11.
5. Aier I, Semwal R, Sharma A, Varadwaj PK. A systematic assessment of statistics, risk factors, and underlying features involved in pancreatic cancer. Cancer epidemiology. 2019 Feb 1;58:104-10.
6. Sarantis P, Koustas E, Papadimitropoulou A, Papavassiliou AG, Karamouzis MV. Pancreatic ductal adenocarcinoma: Treatment hurdles, tumor microenvironment and immunotherapy. World journal of gastrointestinal oncology. 2020 Feb 2;12(2):173.
7. Vincent A, Herman J, Schulick R, Hruban RH, Goggins M. Pancreatic cancer. The lancet. 2011 Aug 13;378(9791):607-20.
8. Siegel RL, Miller KD, Fuchs HE, Jemal A. Cancer statistics, 2021. CA: a cancer journal for clinicians. 2021 Jan;71(1):7-33.
9. Yeh JJ. Prognostic signature for pancreatic cancer: are -we close?.
10. Collisson EA, Sadanandam A, Olson P, Gibb WJ, Truitt M, Gu S, et.al. Subtypes of pancreatic ductal adenocarcinoma and their differing responses to therapy. Nature medicine. 2011

Apr;17(4):500-3.

11. Mizrahi JD, Surana R, Valle JW, Shroff RT. Pancreatic cancer. The Lancet. 2020 Jun 27;395(10242):2008-20.
12. Jaffee EM, Hruban RH, Canto M, Kern SE. Focus on pancreas cancer. Cancer cell. 2002 Jul 1;2(1):25-8.
13. Middleton G, Silcocks P, Cox T, Valle J, Wadsley J, Propper D, et.al. Gemcitabine and capecitabine with or without telomerase peptide vaccine GV1001 in patients with locally advanced or metastatic pancreatic cancer (TeloVac): an open-label, randomised, phase 3 trial. The Lancet Oncology. 2014 Jul 1;15(8):829-40.
14. Giuliani F, Di Maio M, Colucci G, Perrone F. Conventional chemotherapy of advanced pancreatic cancer. Current drug targets. 2012 Jun 1;13(6):795-801.
15. Conroy T, Desseigne F, Ychou M, Bouché O, Guimbaud R, Bécouarn Y, Adenis A, et.al. FOLFIRINOX versus gemcitabine for metastatic pancreatic cancer. New England journal of medicine. 2011 May 12;364(19):1817-25.
16. Von Hoff DD, Ervin T, Arena FP, Chiorean EG, Infante J, Moore M, et.al. Increased survival in pancreatic cancer with nab-paclitaxel plus gemcitabine. New England journal of medicine. 2013 Oct 31;369(18):1691-703.
17. Moertel CG. Clinical management of advanced gastrointestinal cancer. Cancer. 1975 Aug;36(S2):675-82.
18. Sinn M, Bahra M, Liersch T, Gellert K, Messmann H, Bechstein W, et.al. CONKO-005: adjuvant chemotherapy with gemcitabine plus erlotinib versus gemcitabine alone in patients after R0 resection of pancreatic cancer: a multicenter randomized phase III trial. Journal of Clinical Oncology. 2017 Oct 10;35(29):3330-7.
19. Moore MJ, Goldstein D, Hamm J, Figer A, Hecht JR, Gallinger S, et.al. Erlotinib plus gemcitabine compared with gemcitabine alone in patients with advanced pancreatic cancer: a phase III trial of the National Cancer Institute of Canada Clinical Trials Group. Journal of clinical oncology. 2007 May 20;25(15):1960-6.
20. Goggins M. Identifying molecular markers for the early detection of pancreatic neoplasia. InSeminars in oncology 2007 Aug 1 (Vol. 34, No. 4, pp. 303-310). WB Saunders.
21. Kolbert CP, Chari S, Sreekumar R. Microarray technologies for gene transcript analysis in pancreatic cancer. Technology in cancer research & treatment. 2008 Feb;7(1):55-9.
22. Grützmann R, Boriss H, Ammerpohl O, Lüttges J, Kalthoff H, Schackert HK, et.al. Meta-analysis of microarray data on pancreatic cancer defines a set of commonly dysregulated genes. Oncogene. 2005 Jul;24(32):5079-88.
23. Qian Y, Gong Y, Fan Z, Luo G, Huang Q, Deng S, et.al. Molecular alterations and targeted therapy in pancreatic ductal adenocarcinoma. Journal of hematology & oncology. 2020

Dec;13:1-20.

24. Ma J, Sawai H, Ochi N, Matsuo Y, Xu D, Yasuda A, et.al. PTEN regulate angiogenesis through PI3K/Akt/VEGF signaling pathway in human pancreatic cancer cells. Molecular and cellular biochemistry. 2009 Nov;331:161-71.
25. Zhang Y, Zhang J, Xu K, Xiao Z, Sun J, Xu J, Wang J, Tang Q. PTEN/PI3K/mTOR/B7-H1 signaling pathway regulates cell progression and immuno-resistance in pancreatic cancer. Hepato-gastroenterology. 2013 Oct 1;60(127):1766-72.
26. Melstrom LG, Salabat MR, Ding XZ, Milam BM, Strouch M, Pelling JC, Bentrem DJ. Apigenin inhibits the GLUT-1 glucose transporter and the phosphoinositide 3-kinase/Akt pathway in human pancreatic cancer cells. Pancreas. 2008 Nov 1;37(4):426-31.
27. Liu Y, Ao X, Ding W, Ponnusamy M, Wu W, Hao X, Yu W, Wang Y, Li P, Wang J. Critical role of FOXO3a in carcinogenesis. Molecular cancer. 2018 Dec;17:1-2.
28. Barrett T, Wilhite SE, Ledoux P, Evangelista C, Kim IF, Tomashevsky M, Marshall KA, Phillippy KH, Sherman PM, Holko M, Yefanov A. NCBI GEO: archive for functional genomics data sets—update. Nucleic acids research. 2012 Nov 26;41(D1):D991-5.
29. Benjamini Y, Hochberg Y. Controlling the false discovery rate: a practical and powerful approach to multiple testing. Journal of the Royal statistical society: series B (Methodological). 1995 Jan;57(1):289-300.
30. Laskowski RA, Rullmann JA, MacArthur MW, Kaptein R, Thornton JM. AQUA and PROCHECK-NMR: programs for checking the quality of protein structures solved by NMR. Journal of biomolecular NMR. 1996 Dec;8:477-86.
31. Geourjon C, Deleage G. SOPMA: significant improvements in protein secondary structure prediction by consensus prediction from multiple alignments. Bioinformatics. 1995 Dec 1;11(6):681-4.
32. Hirokawa T, Boon-Chieng S, Mitaku S. SOSUI: classification and secondary structure prediction system for membrane proteins. Bioinformatics (Oxford, England). 1998;14(4):378-9.
33. Schwede T, Kopp J, Guex N, Peitsch MC. SWISS-MODEL: an automated protein homology-modeling server. Nucleic acids research. 2003 Jul 1;31(13):3381-5.
34. Laskowski RA, Rullmann JA, MacArthur MW, Kaptein R, Thornton JM. AQUA and PROCHECK-NMR: programs for checking the quality of protein structures solved by NMR. Journal of biomolecular NMR. 1996 Dec;8:477-86.
35. Pettersen EF, Goddard TD, Huang CC, Couch GS, Greenblatt DM, Meng EC, Ferrin TE. UCSF Chimera—a visualization system for exploratory research and analysis. Journal of computational chemistry. 2004 Oct;25(13):1605-12.
36. Guex N, Peitsch MC. SWISS-MODEL and the Swiss-Pdb Viewer: an environment for

comparative protein modeling. electrophoresis. 1997;18(15):2714-23.

37. Kim S, Chen J, Cheng T, Gindulyte A, He J, He S, Li Q, Shoemaker BA, Thiessen PA, Yu B, Zaslavsky L. PubChem in 2021: new data content and improved web interfaces. Nucleic acids research. 2021 Jan 8;49(D1):D1388-95.
38. Lipinski CA. Drug-like properties and the causes of poor solubility and poor permeability. Journal of pharmacological and toxicological methods. 2000 Jul 1;44(1):235-49.
39. Halgren TA, Murphy RB, Friesner RA, Beard HS, Frye LL, Pollard WT, Banks JL. Glide: a new approach for rapid, accurate docking and scoring. 2. Enrichment factors in database screening. Journal of medicinal chemistry. 2004 Mar 25;47(7):1750-9.
40. Hanwell MD, Curtis DE, Lonie DC, Vandermeersch T, Zurek E, Hutchison GR. Avogadro: an advanced semantic chemical editor, visualization, and analysis platform. Journal of cheminformatics. 2012 Dec;4:1-7.
41. O'Boyle NM, Banck M, James CA, Morley C, Vandermeersch T, Hutchison GR. Open Babel: An open chemical toolbox. Journal of cheminformatics. 2011 Dec;3:1-4.
42. BIOVIA DS. Discovery Studio, version 24.1. 0.23298. Dassault Systèmes: San Diego, CA, USA. 2024.
43. Jones S, Rappoport JZ. Interdependent epidermal growth factor receptor signalling and trafficking. The international journal of biochemistry & cell biology. 2014 Jun 1;51:23-8.
45. Oliveira-Cunha M, Newman WG, Siriwardena AK. Epidermal growth factor receptor in pancreatic cancer. Cancers. 2011 Mar 24;3(2):1513-26.
46. Xiong HQ, Abbruzzese JL. Epidermal growth factor receptor-targeted therapy for pancreatic cancer. InSeminars in oncology 2002 Oct 1 (Vol. 29, No. 5, pp. 31-37). WB Saunders.
47. Ueda S, Ogata S, Tsuda H, Kawarabayashi N, Kimura M, Sugiura Y, Tamai S, Matsubara O, Hatsuse K, Mochizuki H. The correlation between cytoplasmic overexpression of epidermal growth factor receptor and tumor aggressiveness: poor prognosis in patients with pancreatic ductal adenocarcinoma. Pancreas. 2004 Jul 1;29(1):e1-8.
48. Navas C, Hernández-Porras I, Schuhmacher AJ, Sibilia M, Guerra C, Barbacid M. EGF receptor signaling is essential for k-ras oncogene-driven pancreatic ductal adenocarcinoma. Cancer cell. 2012 Sep 11;22(3):318-30.
49. Xiong HQ, Rosenberg A, LoBuglio A, Schmidt W, Wolff RA, Deutsch J, Needle M, Abbruzzese JL. Cetuximab, a monoclonal antibody targeting the epidermal growth factor receptor, in combination with gemcitabine for advanced pancreatic cancer: a multicenter phase II Trial. Journal of clinical oncology. 2004 Jul 1;22(13):2610-6.
50. Glauser DA, Schlegel W. The emerging role of FOXO transcription factors in pancreatic β cells. Journal of Endocrinology. 2007 May 1;193(2):195-207.
51. Kumazoe M, Takai M, Bae J, Hiroi S, Huang Y, Takamatsu K, Won Y, Yamashita M, Hidaka

S, Yamashita S, Yamada S. FOXO3 is essential for CD44 expression in pancreatic cancer cells. Oncogene. 2017 May;36(19):2643-54.

52. Hajri A, Coffy S, Vallat F, Evrard S, Marescaux J, Aprahamian M. Human pancreatic carcinoma cells are sensitive to photodynamic therapy in vitro and in vivo. British Journal of Surgery. 1999 Jul 1;86(7):899-906.
53. Evrard S, Keller P, Hajri A, Balboni G, Mendoza-Burgos L, Damgé C, Marescaux J, Aprahamian M. Experimental pancreatic cancer in the rat treated by photodynamic therapy. Journal of British Surgery. 1994 Aug;81(8):1185-9.
54. He X, Wang N, Zhang Y, Huang X, Wang Y. The therapeutic potential of natural products for treating pancreatic cancer. Frontiers in Pharmacology. 2022 Nov 2;13:1051952.
55. Tomeh MA, Hadianamrei R, Zhao X. A review of curcumin and its derivatives as anticancer agents. International journal of molecular sciences. 2019 Feb 27;20(5):1033.
56. Rahmani AH, Al Zohairy MA, Aly SM, Khan MA. Curcumin: a potential candidate in prevention of cancer via modulation of molecular pathways. BioMed research international. 2014;2014(1):761608.
57. Xie X, Yu T, Li X, Zhang N, Foster LJ, Peng C, Huang W, He G. Recent advances in targeting the “undruggable” proteins: from drug discovery to clinical trials. Signal transduction and targeted therapy. 2023 Sep 6;8(1):335.
58. O'Neil NJ, Bailey ML, Hieter P. Synthetic lethality and cancer. Nature Reviews Genetics. 2017 Oct;18(10):613-23.
59. Wang S, Zheng Y, Yang F, Zhu L, Zhu XQ, Wang ZF, Wu XL, Zhou CH, Yan JY, Hu BY, Kong B. The molecular biology of pancreatic adenocarcinoma: translational challenges and clinical perspectives. Signal transduction and targeted therapy. 2021 Jul 5;6(1):249.